EUROPEAN SOUTHERN OBSERVATORY

Organisation Européenne pour des Recherches Astronomiques dans l'Hémisphere Austral
Europäische Organisation für astronomische Forschung in der südlichen Hemisphäre

VERY LARGE TELESCOPE

PRIMA Metrology Test Report

Doc. No. VLT-TRE-ESO-15730-4042
Issue 1
Date 02/04/2008

	Name	Date	Signature
Prepared	S. Leveque/N.Schuler		
Approved	F.Delplancke		
Released	R.Gilmozzi		

Change Record

Issue / Rev.	Date	Section / Page. affected	Reason/Remarks
1	02/04/2008	all	Issued for PRIMA PAE

Table of Contents

1 Scope

This document compiles the results obtained during the integration and test of the PRIMA Metrology System in Garching. For a description of the metrology system and of its measurement principle, the reader shall refer to RD 2.

2 Reference Documents

RD 1 VLT-LIS-ESO-15730-2995, Issue 2, Configuration Item Data List for the PRIMA Metrology System

RD 2 VLT-TRE-ESO-15730-3000, Issue 2, Design Description of the PRIMA Metrology System.

RD 3 VLT-ICD-ESO-15730-2922, Issue 1, VLTI PRIMA Interface Control Document between the Metrology System and the AT Star Separator

RD 4 VLT-TRE-ESO-15732-4087,Issue 1, Design of the Pupil Tracker for PRIMET

RD 5 VLT-TRE-ESO-15730-3799, Issue 1, Specifications for high sensitive 4-quadrant detectors for the PRIMA Metrology System

RD 6 VLT-TRE-ESO-15732-4542, issue 1, Performance of the Metrology Pupil tracking measured on STS#AT1in Garching

RD 7 VLT-TRE-ESO-15731-3884, Issue 1, Test of the laser frequency stabilization system of the PRIMA Metrology System

RD 8 VLT-TRE-IMT-15374-3726, Issue 1, As built Phase Meter configuration for the PRIMA Metrology System

RD 9 VLT-TRE-ESO-15735-2963, Issue 1, Design of the Control Electronics of the PRIMA Metrology System

RD 10 VLT-SPE-ESO-15736-3899, Issue 1, Specification for the PRIMA Metrology data files, data logging and algorithms

RD 11 VLT-MAN-ESO-15734-4535, issue 1,Modifications of the phasemeter firmware.

RD 12 VLT-TRE-ESO-15740-4570, issue 1, 05/08/2008, FSU 6-pixel Measured performance, calibration and fringe tracking.

3 Introduction

The conventions used by the PRIMA Metrology are reported in the following table according to RD 10.

Table 1 Allocation of the Metrology channels and heterodyne frequencies to the VLTI instruments and input channels. (ν laser optical frequency)

<table>
<tr><th colspan="2">Channel A (FSU A)</th><th colspan="2">Channel B (FSU B)</th></tr>
<tr><td>IP3</td><td>IP1</td><td>IP4</td><td>IP2</td></tr>
<tr><td>ν + 38.65 MHz</td><td>ν + 38 MHz</td><td>ν - 39.55 MHz</td><td>ν - 40 MHz</td></tr>
<tr><td>Polarization: P</td><td>Polarization: S</td><td>Polarization: P</td><td>Polarization: S</td></tr>
<tr><td colspan="2">f_a = 650 kHz
OPD_a = IP3 -IP1 >0</td><td colspan="2">f_b = 450 kHz
OPD_b = IP4 - IP2 > 0
(also used for phase compensation)</td></tr>
<tr><td colspan="4">$\Delta\nu$ = 78 MHz</td></tr>
<tr><td colspan="4">$f_a - f_b$ = 200 kHz
$\Delta L = OPD_a - OPD_b$ =Ip3-Ip1-Ip4+Ip2> 0</td></tr>
</table>

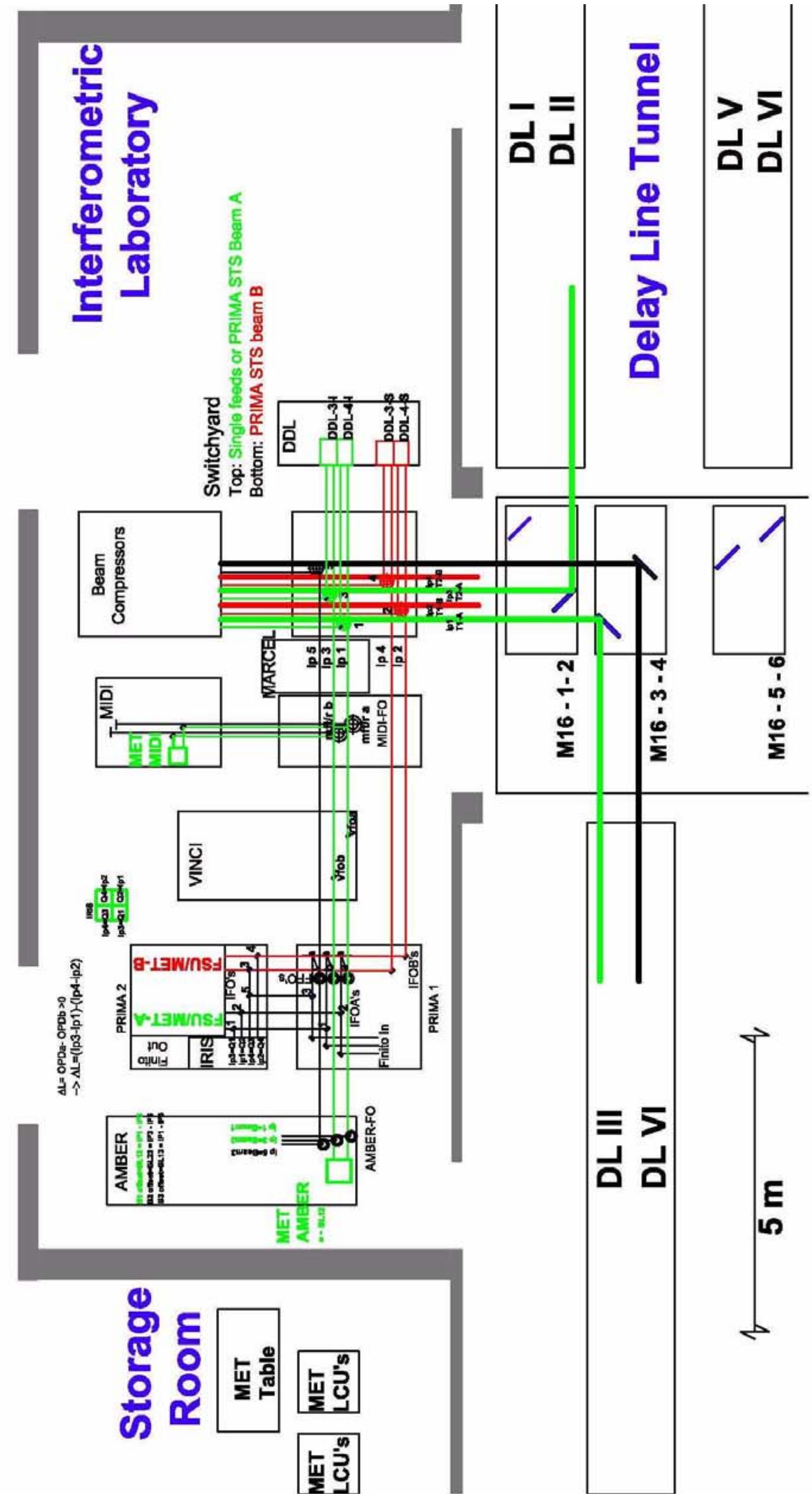

Figure 1 *Overview of the location of the metrology hardware: 1 optical table and 2 electronic cabinets are located inside the storage room. Four beam launcher/combiner areas inside the interferometric laboratory located on the Amber, FSU#A, FSU#B and MIDI tables.*

4 Heterodyne assembly

4.1 Acousto Optics Modulators

The phase detection, based on superheterodyne detection, requires to use two pairs of slightly different optical frequencies. These optical frequencies are generated by four fiber pigtailed acousto-optic modulators (AOM). The efficiency of the frequency shifting depends on the amplitude of the acoustic modulation signal, thus it depends on the amplitude of the electric signal feeding the modulator. This amplitude is optimized and the transmission of the AOM is measured. This transmission includes the connection loss of the input fiber.

Table 2 Transmission of the AOM and optimal amplitude of the modulation signal. The input power was 24.8 mW

AOM serial number	Output Power (mW)	Transmission (%)	Optimal amplitude[1] of the modulation signal (V)
417649 -40.00 MHz	18.6	75	37.6
417650 -39.55 MHz	15.2	61	35
417651 38.00 MHz	17.8	71	34.4
417652 38.65 MHz	20.2	81	35

1. pk-pk measured in 1MΩ.

The efficiency of frequency shifting of the AOM is a function of the power of the acoustic-wave in the crystal and presents a maximum. The power in the acoustic wave can be set on the front face of the rf signal generator by a potentiometer or by applying a voltage to the “Analog input” BNC (0-1 V). The effect of applying a voltage to the analog input has been measured and is plot in Figure 2. The normalized intensity as a function of the input voltage can be modeled by a square sine function as predicted by the theory of acousto-optics. Therefore the AOM can be used in the set-up as a variable optical attenuator. The relation voltage /transmission was calculated from the measurements below and are given in RD 10.

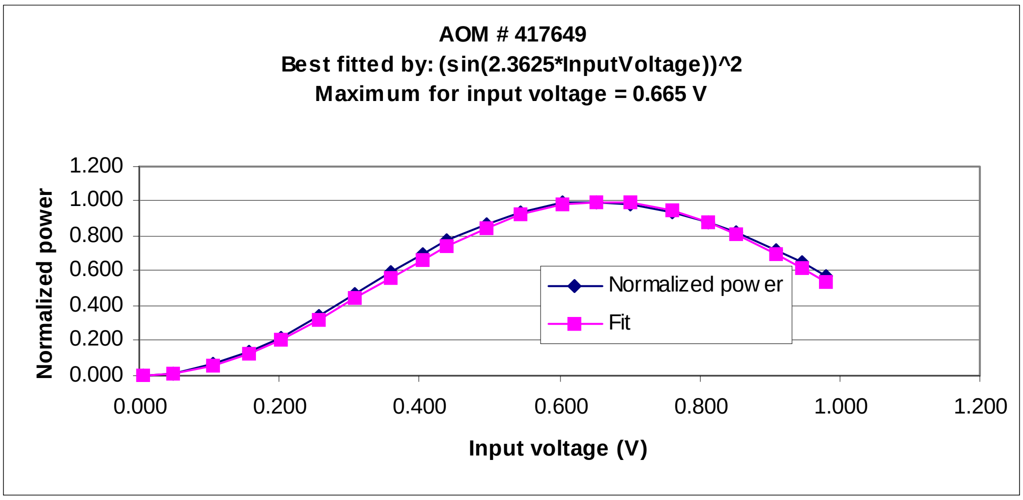

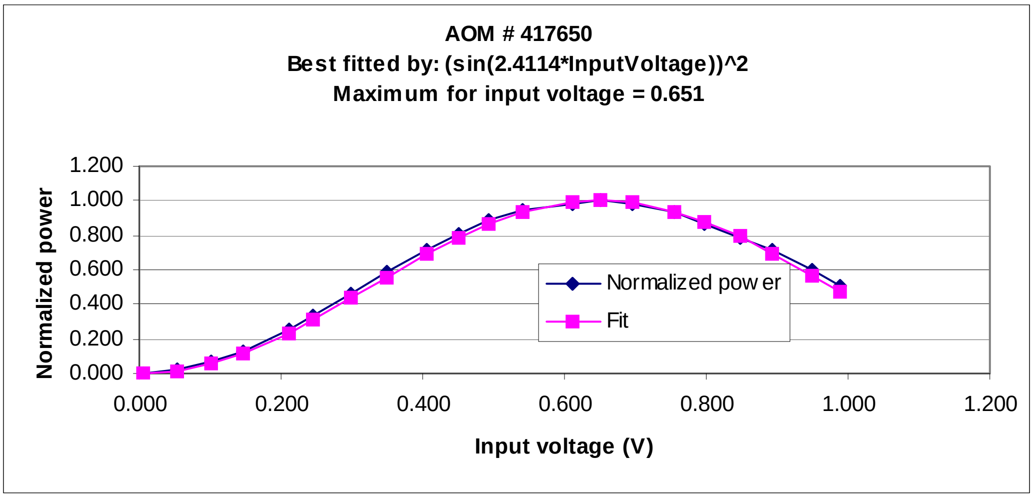

Figure 2 *Normalized power output of the AOM as a function of the voltage applied to the analog input of the rf signal generator.*

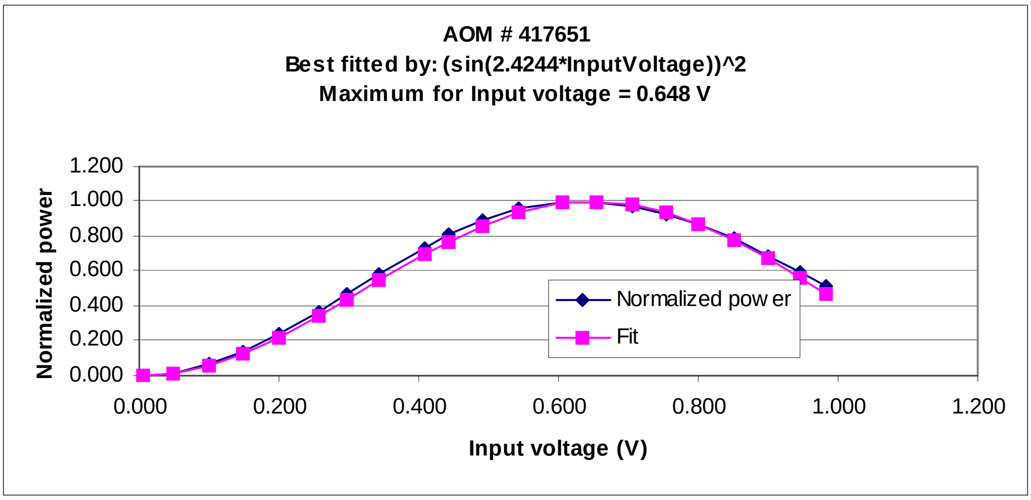

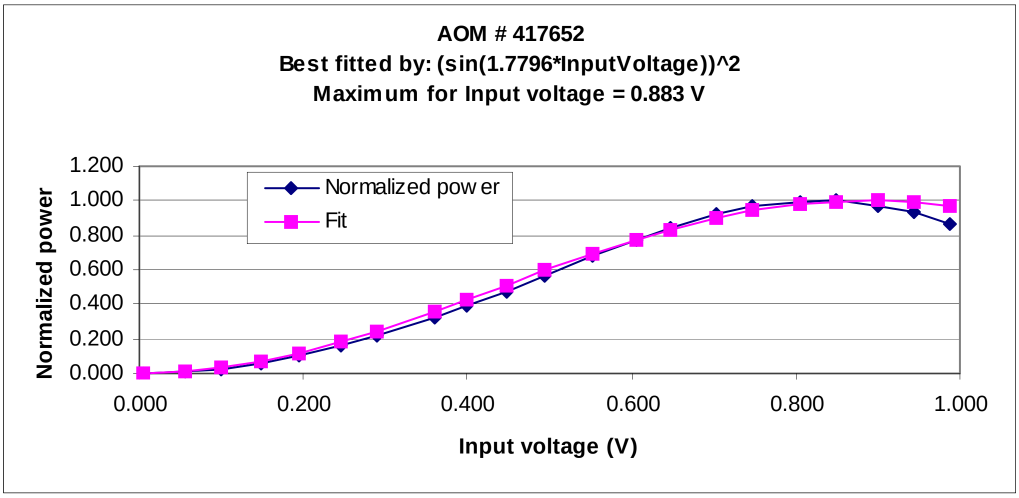

Figure 2 *Normalized power output of the AOM as a function of the voltage applied to the analog input of the rf signal generator.*

The model for the spare drivers are given below:

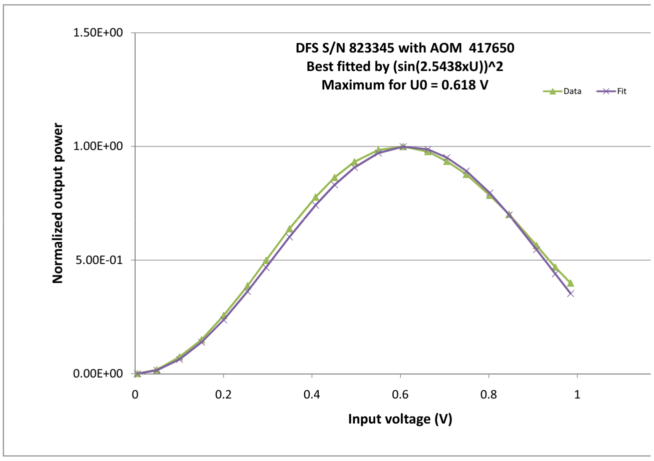

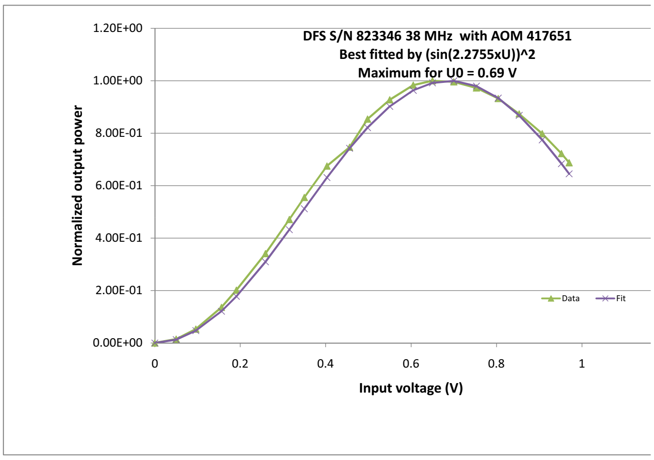

Figure 3 Experimental transmission curves and corresponding models of the AOM with the spare drivers.

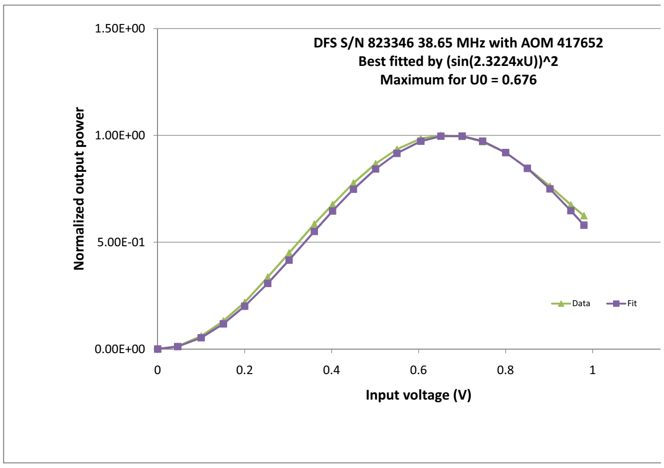

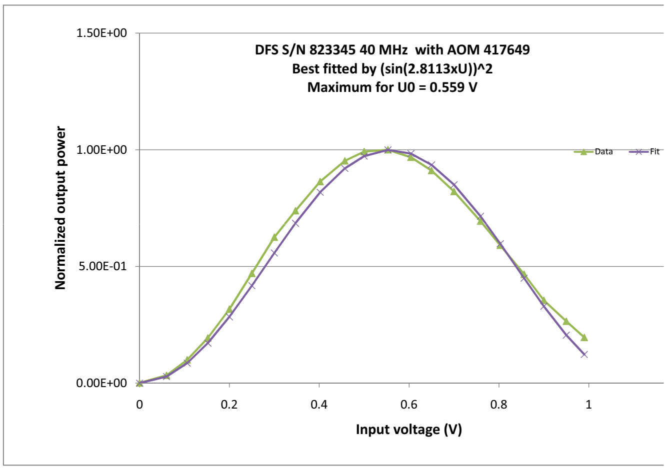

Figure 3 Experimental transmission curves and corresponding models of the AOM with the spare drivers.

4.2 2x4 Fiber coupler

75% of the laser power is dedicated to the interferometer. These 75% must be split in 4 equal parts to create the two pairs of heterodyne frequencies. This is achieved with a 2x4 fiber coupler. Splitting ratio has been already measured in previous tests. The new tests are motivated by the problems discovered on the 25/75 fiber coupler (see Section 4.3). In a first time the power at two outputs of the coupler have been measured without any polarizing optics in the set-up as described in Figure 4. The power ratio between the two outputs is stable within a 1% as visible in Figure 5. A similar measurement has been made with linear polarizers introduced in the two channels after the fiber coupler as in Figure 6. In that case, one observes that the power noise in the two channels is decorrelated and the ratio of the power at the two outputs presents large fluctuations, Figure 7. The power noise is due to the variation of the polarization state.

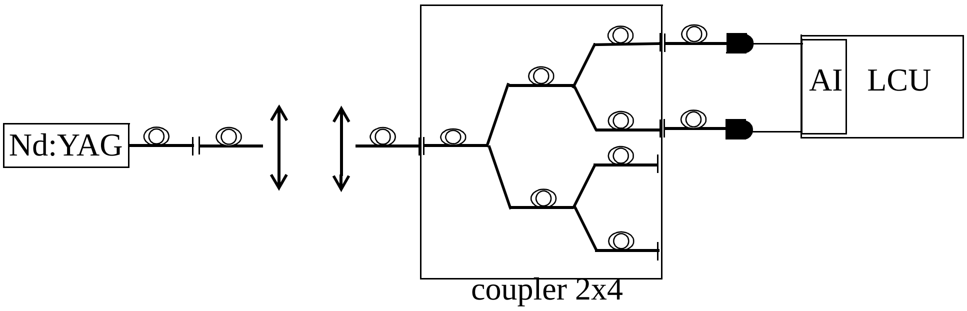

Figure 4 *set-up used to measure the variation of the splitting ratio of the 2x4 fiber coupler. The saturation threshold of the detector is low (~1 μW). Therefore the light is collimated and recoupled into a fibre before the fiber coupler in order to allow a fine tuning of the power.*

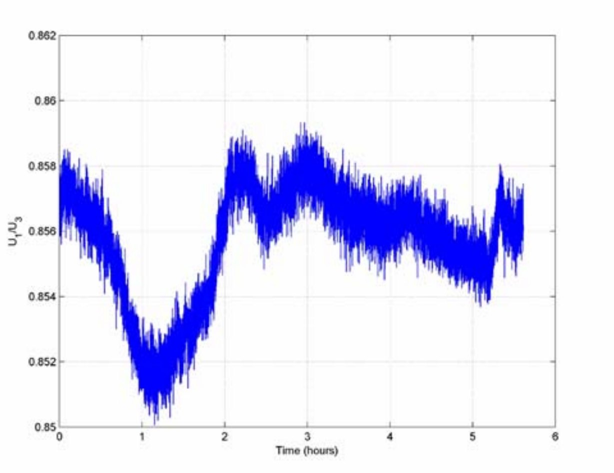

Figure 5 *The power is measured simultaneously at two outputs of the 2x4 coupler in a set-up without any polarizing optics. The ratio of the power measured at the outputs is plotted as a function of time. The standard deviation is 0.18% and the peak-to-peak deviation is 0.93%.*

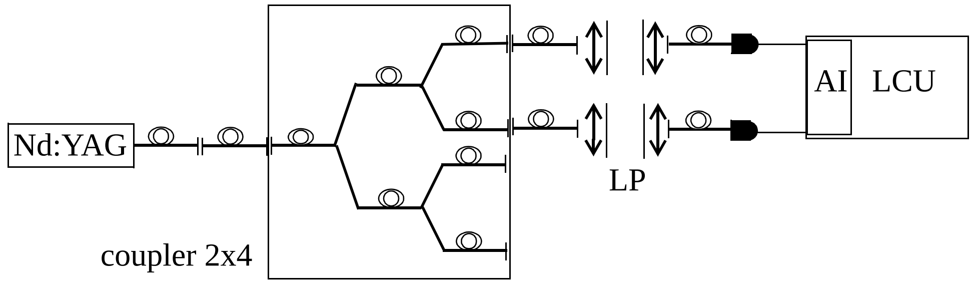

Figure 6 *set-up used to measure the variation of the splitting ratio of the 2x4 fiber coupler when linear polarizers (LP) are introduced after the fiber coupler. The saturation threshold of the detector is low (~1 μW). Therefore the light is collimated and recoupled into a fibre before the fiber coupler in order to allow a fine tuning of the power.*

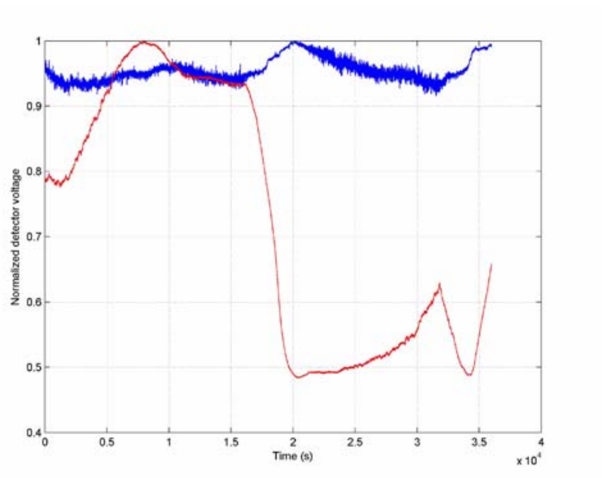

Figure 7 *The power is measured simultaneously after two linear polarizers located at two outputs of the 2x4 coupler. The ratio of the power measured at the outputs is plotted as a function of time.*

The coupler does not introduce power fluctuations but it creates variations of the polarization state. This may be due to the change of mechanical strain on the fiber itself or on the connectors due to the temperature change.

4.3 Fiber coupler 25/75

The power delivered by the Nd:YAG laser is split in two by a fiber coupler with ratio 25% / 75%. 25% are use for the laser frequency stabilization and 75% for the interferometry. The main characteristics of the coupler have been measured. The power at the two outputs called Y75 and Y25 have been measured simultaneously to determine the coupling ratio of the fiber coupler. The set-up used for this measurement is depicted in Figure 8. The measurement is done over 4 hours and the results are plotted in Figure 9.

Several attempts have been made to measure the total loss of the coupler but they have not proven to be repeatable. Indeed, the loss in the coupler are mainly due to the connections. The loss were measured to be between 10% and 50%. According to the specifications the loss in the fiber coupler should be 10%.

These measurements do not include any polarizing optics which is the case of both the heterodyne assembly (linear polarizer) and the laser frequency stabilization system (frequency doubling crystal). Therefore a set-up has been created to measure the impact of the polarization on the intensity noise created by the fiber coupler. The set-up is depicted in Figure 10 and the results are plotted in Figure 11. The splitting ratio of the fiber coupler is constant but variations of the polarization state at the output fibers create intensity noise when any polarizing optics is used downstream of the fiber coupler. These variations happen at very low frequencies and are probably due to the variations of temperatures. Therefore it may be possible to correct for them by tuning the transmission of the AOM as described in Section 4.

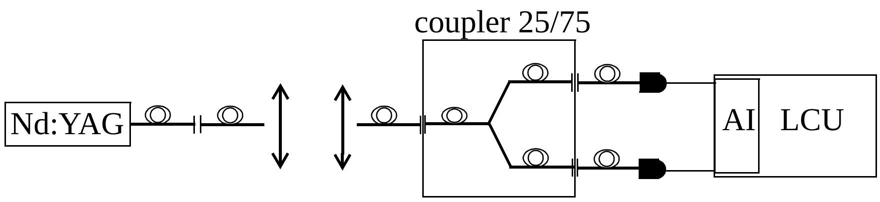

Figure 8 *Set-up used to measure simultaneously the two outputs of the fiber coupler. Two detectors of the phasemeter are used. As they have a really low saturation threshold the power coming out of the laser is decreased by collimating and recoupling the light into a fiber with two OFR fiber ports mounted on an OFR table.*

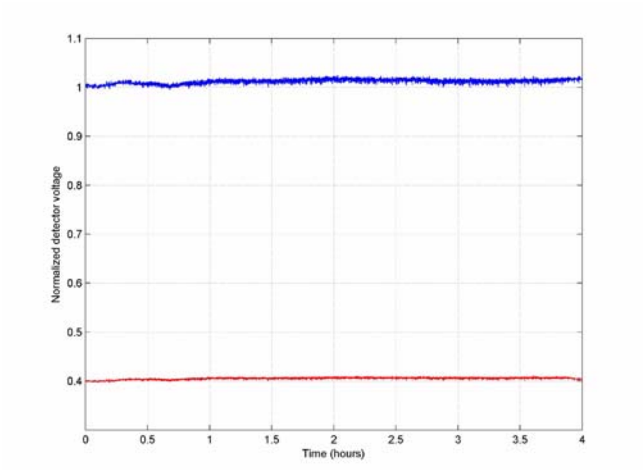

Figure 9 *Left: detector voltages for the two outputs of the fiber coupler (blue: output Y75, red: output Y25).The individual standard deviation are 0.44 V and 0.21 V respectively.*

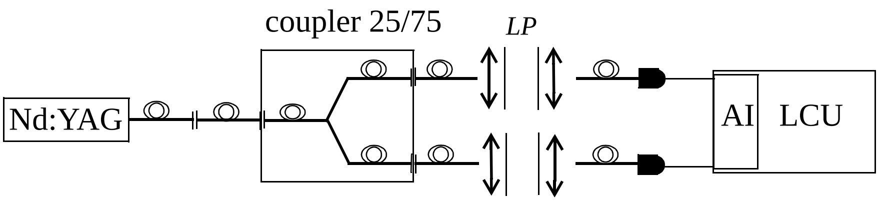

Figure 10 *The power at the two outputs of the 25/75 fiber coupler are measured simultaneously. OFR fiber ports are used to collimate and recouple the light. Linear Polarizers (LP) are used.*

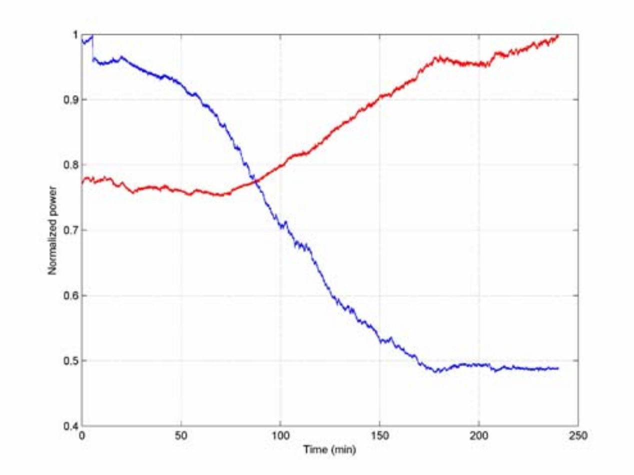

Figure 11 *Normalized detector voltage as a function of time. The standard deviation are 19% and 9% to be compared to less than one percent without polarizing optics (Figure 9).*

5 Laser power and laser frequency Stabilization

The laser used by the metrology is a Innolight Mephisto Nd:YAG laser. The spare laser is a Lightwave 125 Nd:YAG laser. The software is designed to work with both. Both lasers have been characterized.

5.1 Innolight laser

Optical power measured at the output of the Innolight laser Model MIR 500NE-FC (Serial Laser head: 1537 Serial electronics: M330g-0414 Serial Diode A: 95738 Serial Diode B: 84106). Operating conditions (factory set): $T_{crystal}$= deg, I_A=1A, T_A=29.45 °C, I_B=1A, T_B=27.18 °C. At full power the laser emits close to of the transition used for the stabilization for Tcrystal = 27.7 °C. For this temperature the diode current and the laser output power are measured as a function of the voltage fed to the laser driver Power modulation input (located at the back of the laser driver).

Detector: Newport 818-IG

The innolight laser shall be preferably operated at its nominal power (given by the manufacturer). Only in this conditions, the Intensity “noise eater” of the innolight laser delivers optimum performance. Otherwise, some intensity noise will occur at typically fb+/-298 Hz (where fb=650 kHz,or 450 kHz, is the metrology nominal beat signal of the channel under test).

Input voltage U (V)	Diode Current (A)	P(W)
9.98	0.98	0.3192
9.805	0.962	0.304
9.6	0.942	0.2896
9.398	0.922	0.2752
9.191	0.896	0.26
9.004	0.883	0.244
8.801	0.862	0.2288
8.605	0.843	0.2702
8.419	0.825	0.1864
8.201	0.803	0.1592
8.006	0.784	0.132
7.8	0.764	0.104
7.6	0.744	0.072
7.405	0.724	0.04
7.202	0.704	0.0144
7.079	0.692	0.00032
7.006		0

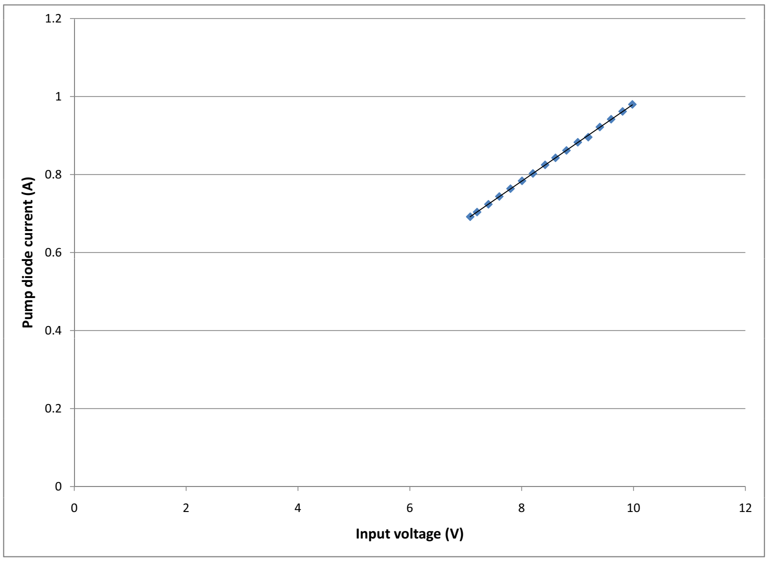

Figure 12 *Current in the pump diode as a function of the voltage applied to the laser driver.*

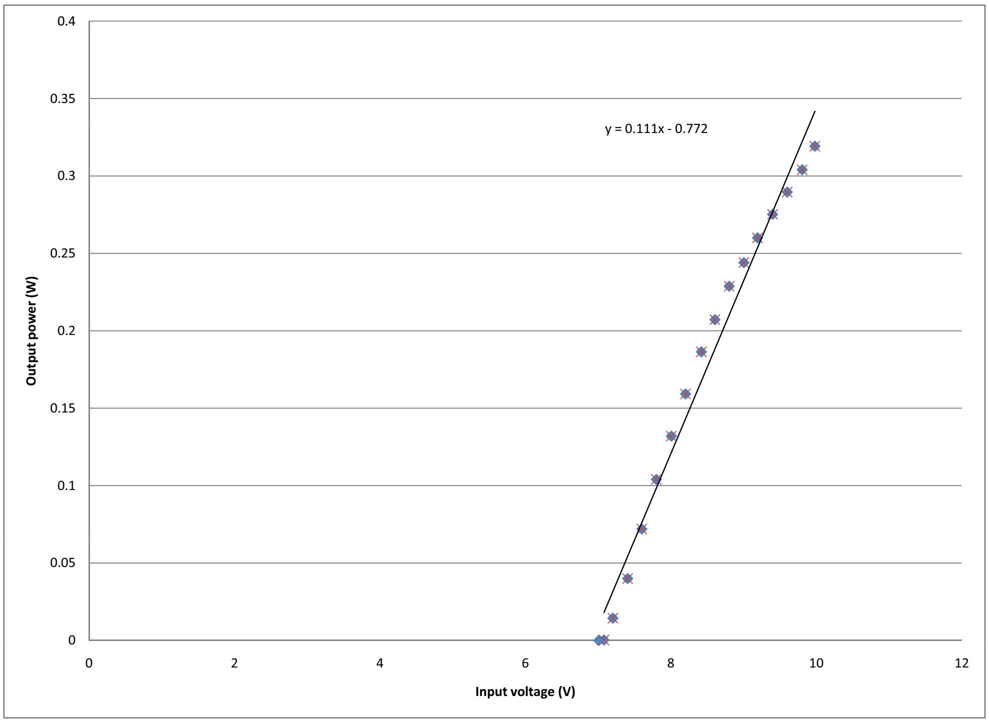

Figure 13 *Power at the output of the laser fiber as a function of the voltage applied to the laser driver. The lasing threshold is 6.935 V, and the voltage required to provide 250 mW is 9.06 V.*

The voltage applied to the laser driver by the analog out board must be limited to 0-10V and is calculated with:

$$P(W) = 0 \Rightarrow U = 0 \tag{5.1-1}$$

$$P(W) > 0 \Rightarrow U = \frac{P(W)}{\alpha} + U_0 . \tag{5.1-2}$$

where $\alpha = 0.111$ and $U_0 = 6.955$.

These formula are implemented in the software module controlling the laser (pmlss).

5.2 Lightwave laser (spare)

Current in A	Optical Power in W
0.6	1.00E-08
0.7	1.62E-08
0.75	1.97E-08
0.8	2.37E-08
0.85	3.20E-08
0.86	4.50E-08
0.865	9.00E-04
0.866	2.00E-03
0.9	1.96E-02
1	7.33E-02
1.015	8.33E-02
1.1	1.29E-01
1.173	1.67E-01
1.2	1.80E-01
1.25	2.02E-01
1.3	2.16E-01
1.35	2.34E-01
1.4	2.57E-01
1.45	2.80E-01
1.457 (LIMIT)	2.82E-01

The power at the output of the laser fiber can be modulated by applying a voltage to the “Output adjust” plug located on the front face of the laser driver. This setting overrides the Power Adjust signal generated internally by the laser driver. The effect of the voltage (-10 V / +2 V) has been measured. The results are plotted in Figure 14. The power as a function of the input voltage (U) can be modeled by:

$$P(W) = \begin{cases} 0.053, & U < -6V \\ U \times 0.0156 + 0.146, & -6V < U < 2V \end{cases} . \quad (5.2\text{-}1)$$

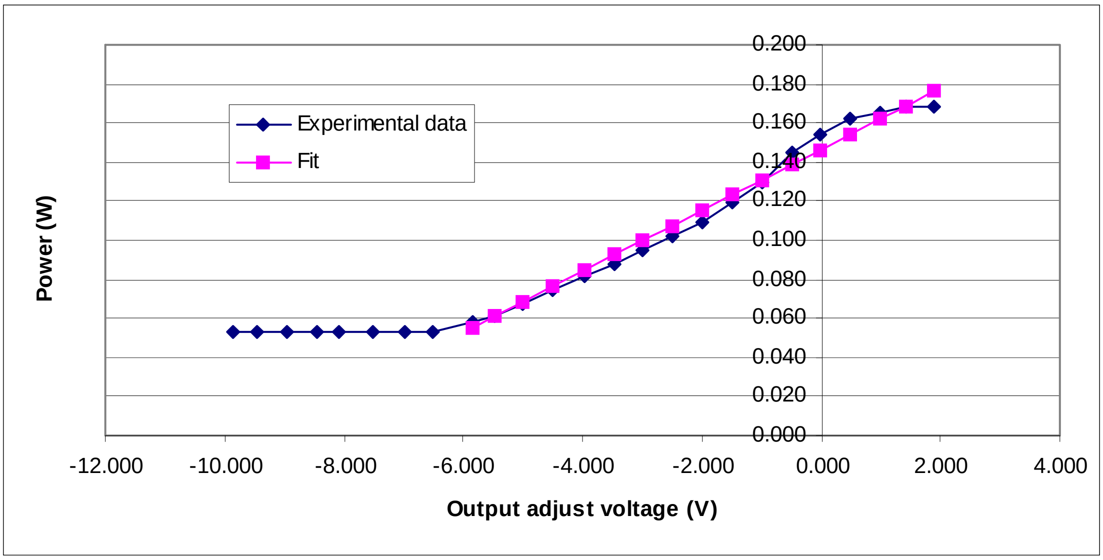

Figure 14 Power at the output of the laser fiber as a function of the voltage fed to the "adjust output" of the laser driver. The laser is initially set to its maximum with the knob of the laser driver.

5.3 Laser frequency stabilization

The measured performance are detailed in RD 7 and illustrated in Fig. 15.
Over 30 min, the open loop frequency excursion is: σ_f =7.4 MHz rms; Δ_f = 22 MHz (P-V)
In the best case, the frequency excursion in closed loop was reduced to:

σ_f = 0.126 MHz rms; Δ_f = 0.892 MHz (P-V)

In all cases, the specification of σ_f =2.27 MHz rms was reached (i.e relative frequency error of $d\nu/\nu=10^{-8}$).

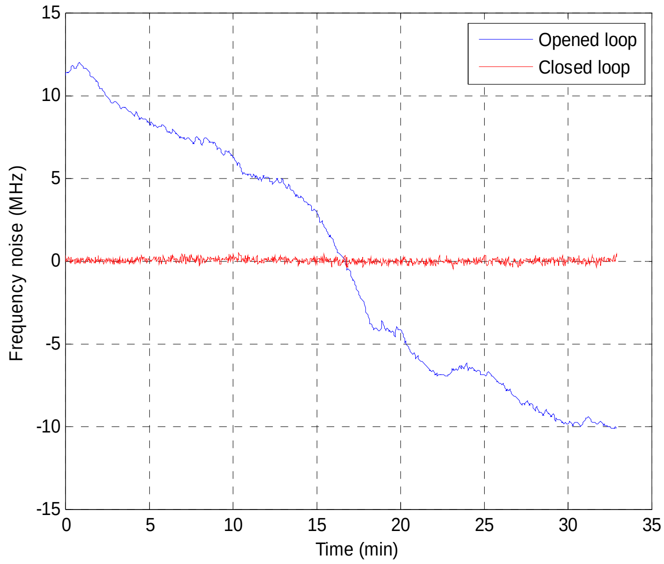

Figure 15 *Performance of the frequency stabilization loop.Best case (see File 16_03_02 reported in table 14.1 of* RD 7)

6 Opto-mechanics

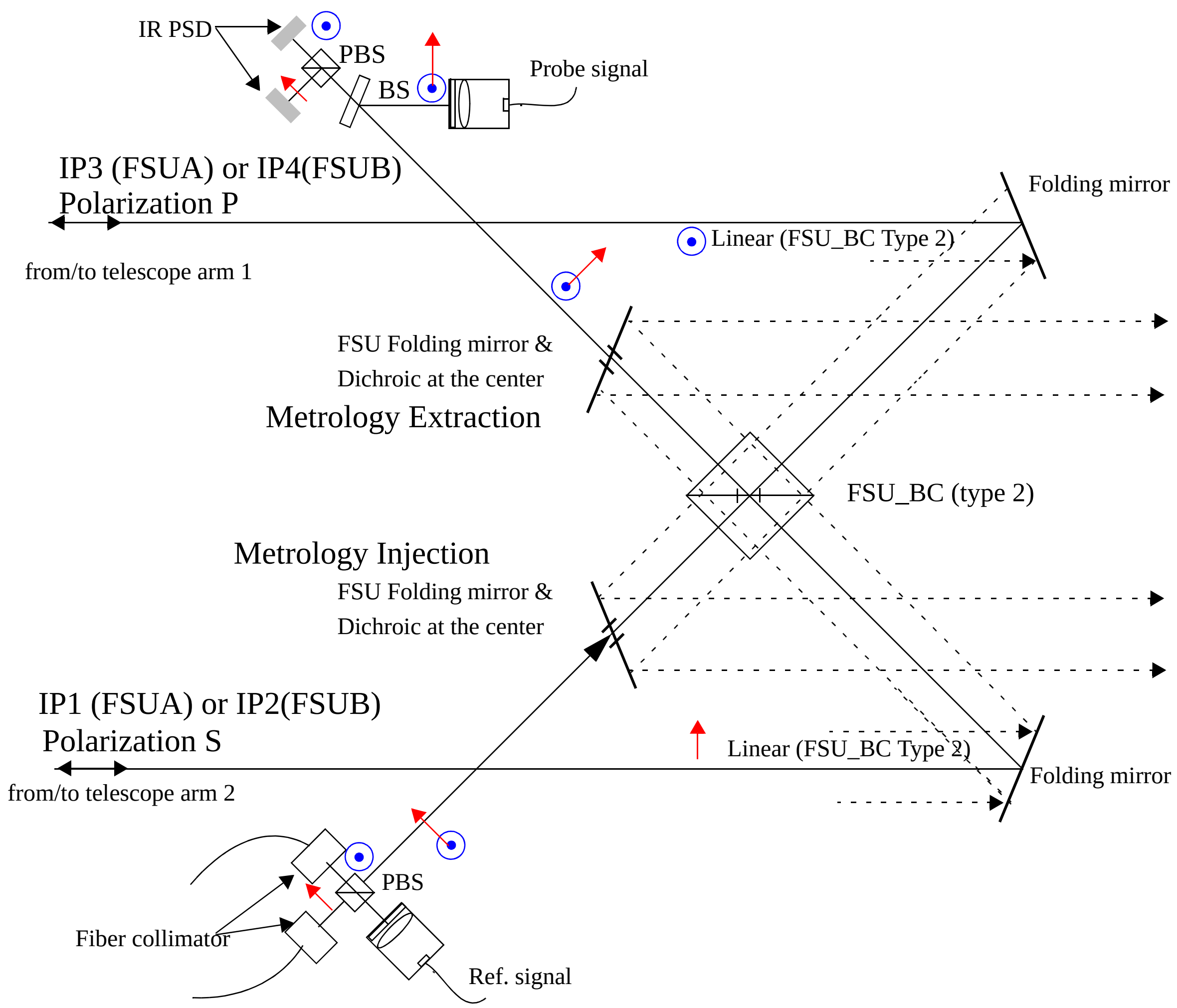

Figure 16 Optical Configuration of the metrology beams for each FSU Channel.The solid lines represent the path followed by the metrology beams. The dotted lines represent the path of the stellar beams in the FSU beam combiner.

6.1 Test of the FSU beam combiner

The portion of the FSU Beam combiner used by the metrology is made of a 50/50 beam splitter (at 1319nm). In addition, 2 linear polarizers with orthogonal orientations are glued on its side to select the P and S components of the metrology beams.

The transmission of the two Beam Combiner has been measured for both input polarizations. The set-up is described in Figure 17. The opto mechanics of the metrology injection is used. Two 1 mm diameter collimated beams are generated from the output of two SM-PM fibers. Two linear polarizers are used to generate perpendicular linear polarization states. The two beams are then superimposed with a polarizing beam splitter. All this opto mechanics is mounted on a translation stage and a goniometer to control the two translations of the beam, the tip and tilt and the rotation of the polarization axis. The beam propagates through a first beam splitter is then aligned with the BC, i.e the beam enters through the coated patch and exits through the two linear polarizers. The transmission and reflection ratio of the first BS are calibrated. This allows to measure the intensity reflected by the BS and deduce the intensity at the input of the BC. This is done so that simultaneous measurements of the intensity are made before and after the BC in order to be insensitive to the laser intensity noise. Due to the small size of the detectors focusing lenses are used.

First the orientation of the input P polarization is adjusted to maximize the transmission of the P polarization (Tp). Then rp is measured in the same configuration.

In a second step, the orientation of the input S polarization is adjusted to maximize the Reflection of the S polarization (Rs). Then ts is measured in this configuration.

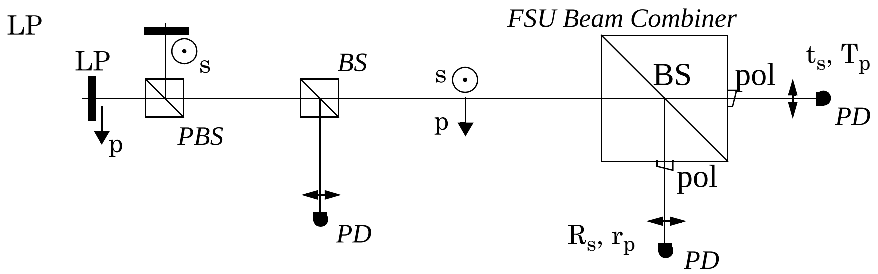

Figure 17 *Set-up for the measurement of the BC transmission and reflection coefficients. LP: Linear Polarizers. (P)BS: (Polarizing) Beam Splitter. BC: Beam Combiner. PD: Photo Diode. s and p denote the linear polarization state respectively perpendicular and parallel to the plane of the optical table.*

The beam combiner installed in FSU A is marked with a 3 on its top. The beam combiner coefficient are summarized in Table 3.

Table 3 *Coefficients of transmission of the cube “3” used in FSU A. The symbols R and T represents the coefficients of reflection and transmission respectively. Small letters are used to indicate that the coefficients correspond to leakage. The indices s and p denote the linear polarization state vertical and horizontal to the plane of the table respectively.*

Coefficient	Measurement (%)	Ratios	Comment
$\mathbf{T_p}$	**54.2**	t_s/T_p=0.011	Max. value of Tp and Rs after optimization of the orientation of the input polarization (=compensation of the alignment errors of the BC polarisors)
t_s	0.6		
$\mathbf{R_s}$	**43.5**	r_p/R_s=0.0062	
r_p	0.27		

The above leakage measurements (polarization crosstalk intrinsic to the beam combiner) would lead in theory to a cyclic error of 7nm (PV) or +/-3.5 nm. Considering that this measurement exclude the contribution of the mis-alignment of the FSU_BC polarizer, it shall be seen as the minimum cyclic error in the current configuration.

6.2 Opto mechanical tests on FSU A

When nothing is specified the measurements have been obtained with an intensity in the YAG pump diode laser of 1.011 A.

6.2.1 Reference signal

When the linear polarizers are set in their nominal position, no interference signal can be seen. This is due to the fact that the power transmitted of the s polarization is too low. This can be counterbalanced by rotating the linear polarizer in front of the fiber port to create some leakage. Indeed the projection of the new polarization on the p-axis is transmitted. After optimization of the linear polarizer orientation the **signal contrast is 87%** (U_{min} = 1.5 mV, U_{Max} = 160 mV).

By doing so the state of polarization at the output of the PBS is no more pure s polarization (with the polarizer in its nominal position the extinction ratio after the PBS is 3×10^{-4}, rotated by 15° the extinction ratio is 3×10^{-3}). This has two consequences: it creates additional loss in the Beam Combiner at the level of the polarizing path of the s arm (the incident polarization and the polarizer axis do not match) and it introduces polarization cross-talk.

These measurements were performed after integration of the new OFR fiber ports, offering a better tilt adjustment sensitivity.

6.2.2 FSUA transmission (forward metrology beam and forward+returned beam)

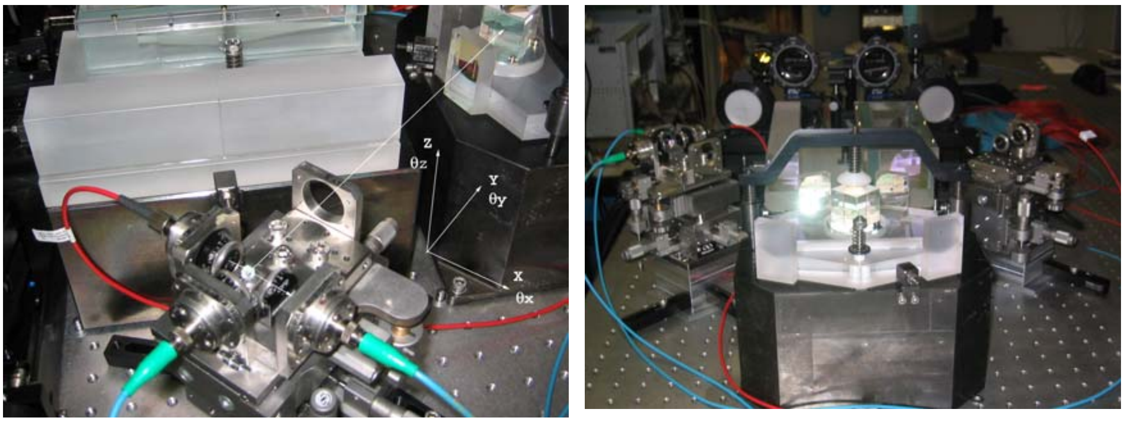

Figure 18 Beam injection (left) and extraction (right) in the FSU

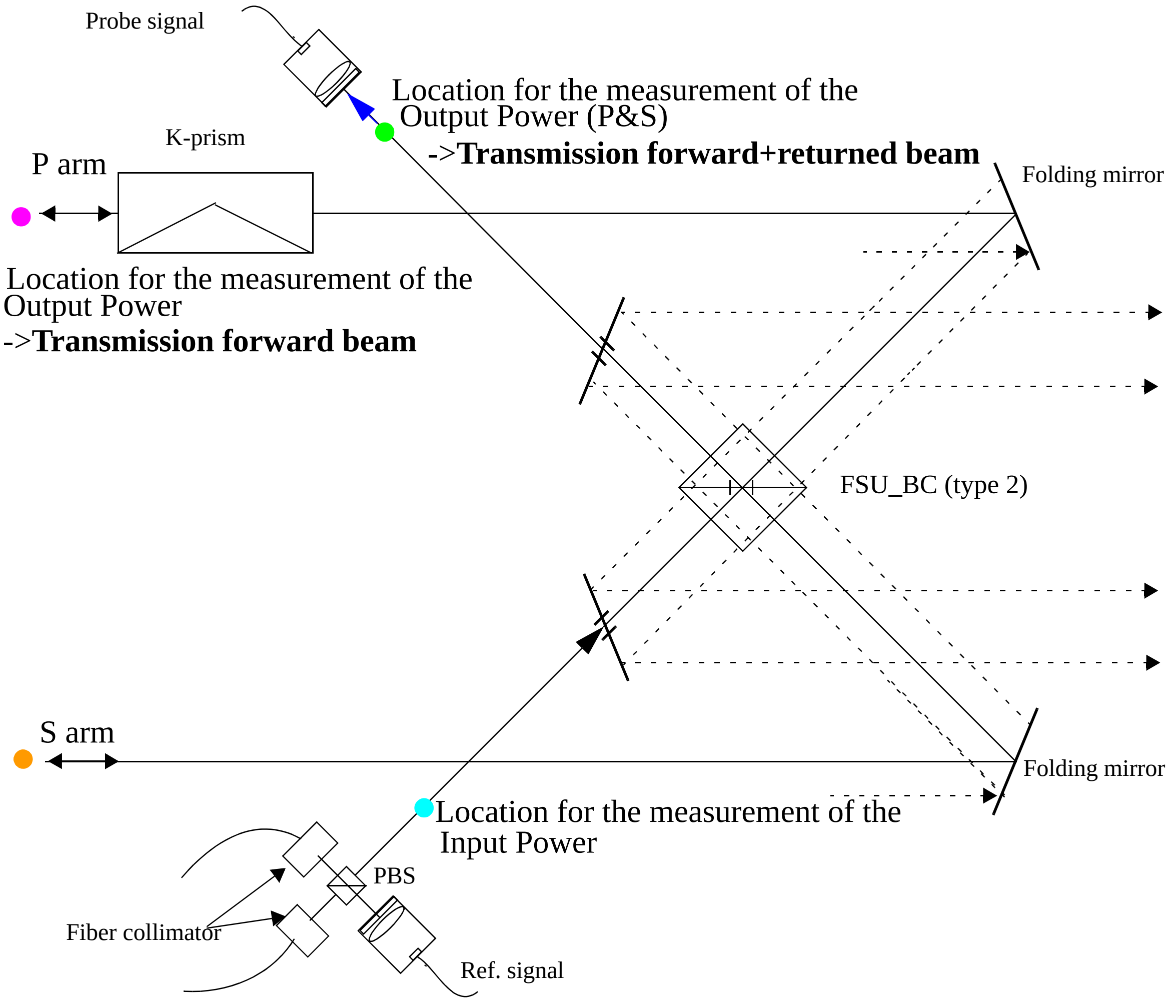

Figure 19 Definition of the measured transmission

*Table 4 “Forward” Transmission of the FSU A in the arm propagating the P polarization (**Ip3**)*

Polarization	Power in (mW)	Power out in P arm (mW)	Transmission (%) 1319nm	ratio in P arm
P	$Ii_p=0.53$	$Io_p=0.260$	**Tp=**Io_p/Ii_p**=49.0**	ts/Tp=0.0037
S	$Ii_s=0.39$	$Io_s=0.0007$	$ts=Io_s/Ii_s=0.18$	$Io_s/Io_p=0.0027$

*Table 5 “Forward” Transmission of the FSU A in the arm propagating the S polarization (**Ip1**)*

Polarization	Power in (mW)	Power out in S arm (mW)	Transmission (%) 1319nm	ratio in S arm
P	Ii_p=0.53	Io_p=0.0005	rp=Io_p/Ii_p=0.09	rp/Rs=0.0024
S	Ii_s=0.39	Io_s=0.147	**Rs**=Io_s/Ii_s=**37.7**	Io_p/Io_s=0.0034

The value of **Tp** and **Rs** shown above are lower than in Table 3. This can be explained as follows:

In Table 3, the orientation of the input polarizations S and P were optimized for maximum throughput (=compensation of the alignment errors of the BC polarisors).

In the case of Table 4 and Table 5, this is not the case anymore:

- the orientation of the input polarizations S and P is adjusted to optimize the contrast of the reference signal
- the overall beam launcher is tilted around θy using its goniometer stage (see Fig. 18) to minimize the polarization leakage

The values of Io_p=0.0005 mW and Io_s=0.0007 mW should be taken with care because they are close to the noise level of the power meter. Therefore, the associated leakage values shown in Table 4 and Table 5 are also biased.

Table 6 Forward+returned “Transmission” through the FSUA and MARCEL (Foward+returned path). The power injected is measured just after the metrology injection opto mechanics and before FSU dichroics with the InGaAs detector (behind an optical density (1/800) and the Newport powermeter. In the table, data are corrected for the attenuation of the optical density. The power transmitted is measured in front of the metrology extraction opto mechanics (after FSU dichroics) with the same detector and powermeter as before.

Input polarization	Power injected (mW)	Power before PRIMET extraction (mW)	FSUA + Marcel transmission (forward + returned path) 1319nm
p	5.6	0.0223	0.4%
s	1.4	0.0077	0.55%
p + s	7.2	0.030	0.42%

6.2.3 Probe signal

Table 7 Probe signal measured at the output of the phasemeter photodiode with an oscilloscope.

Signal frequency (Hz)	650 kHz
U_{min} (V)	0.04
U_{Max} (V)	0.56
U_{mean} (V)	0.300
Contrast (%)	**87**

6.2.4 FSU A Polarization leakage and associated OPD error

The OPD error introduced by polarization leakage has been assessed by 2 methods.
"Method 1" consists in measuring the power of the leakage components in each FSU arm and by computing the expected OPD error as predicted by the theory. Based on Table 8, the error associated with Io_s/ Io_p=0.0073 (p arm) and Io_p/Io_s=0.018 (s arm) is 3.1 nm.
"Method 2" consists in modulating the OPD at a known speed while recording the metrology signal. Any polarization leakage error will appear as a sine wave with a period of λ/2. Results similar to "Method 1" have been obtained.

After careful alignment of the beam launcher orientation by the goniometer, the OPD error introduced by polarization leakage is estimated to reach 3.5 nm 0-Pk for each channel, i.e.7nm 0-Pk for the 2 PRIMET channels.
Considering that the polarization cross-talk error is a sine wave with a period of 1 λ , the associated rms value to be used in the error budget is 7/sqrt(2)=5 nm.

Table 8 Polarization leakage in FSU A. One arm of the interferometer is blocked at a time. The signal detected by the phasemeter is then measured for each input polarization and for both simultaneously to assess the amount of cross-talk created in the interferometer arm that is not blocked. Measurements are with an oscilloscope at the output of the phasemeter photodiode.

Interferomter arm	Input polarization	Output Signal	Ratio
p	Ii_p	DC mean : Io_p=1500 mV	Io_s/ Io_p=0.0073 (depends on Ii_p and Ii_s)
	Ii_s	DC mean : Io_s=11 mV	
	$Ii_{(p+s)}$	mean : 1.53 mV peak-to-peak : 220 mV	
s	Ii_p	DC : mean Io_p=32 mV	Io_p/Io_s=0.018 (depends on Ii_p and Ii_s)
	Ii_s	DC : mean Io_s=1800 mV	
	$Ii_{(p+s)}$	mean : 1800 mV peak-to-peak : 200 mV	

6.2.5 Parasitic reflexion from the K-prism front surface on FSUA

After replacement of the contaminated FSUA folding mirrors and dichroics, some intensity fluctuations appeared in the metrology probe signal. An example of these fluctuations is given in Figure 21 where the DC signals on the phasemeter photodiodes have been recorded over a week-end. One can see that the signal of the probe 650 kHz photodiode present large variations (mean=1.054 V; Peak-to-valley=1.239 V; rms=0.237 V).

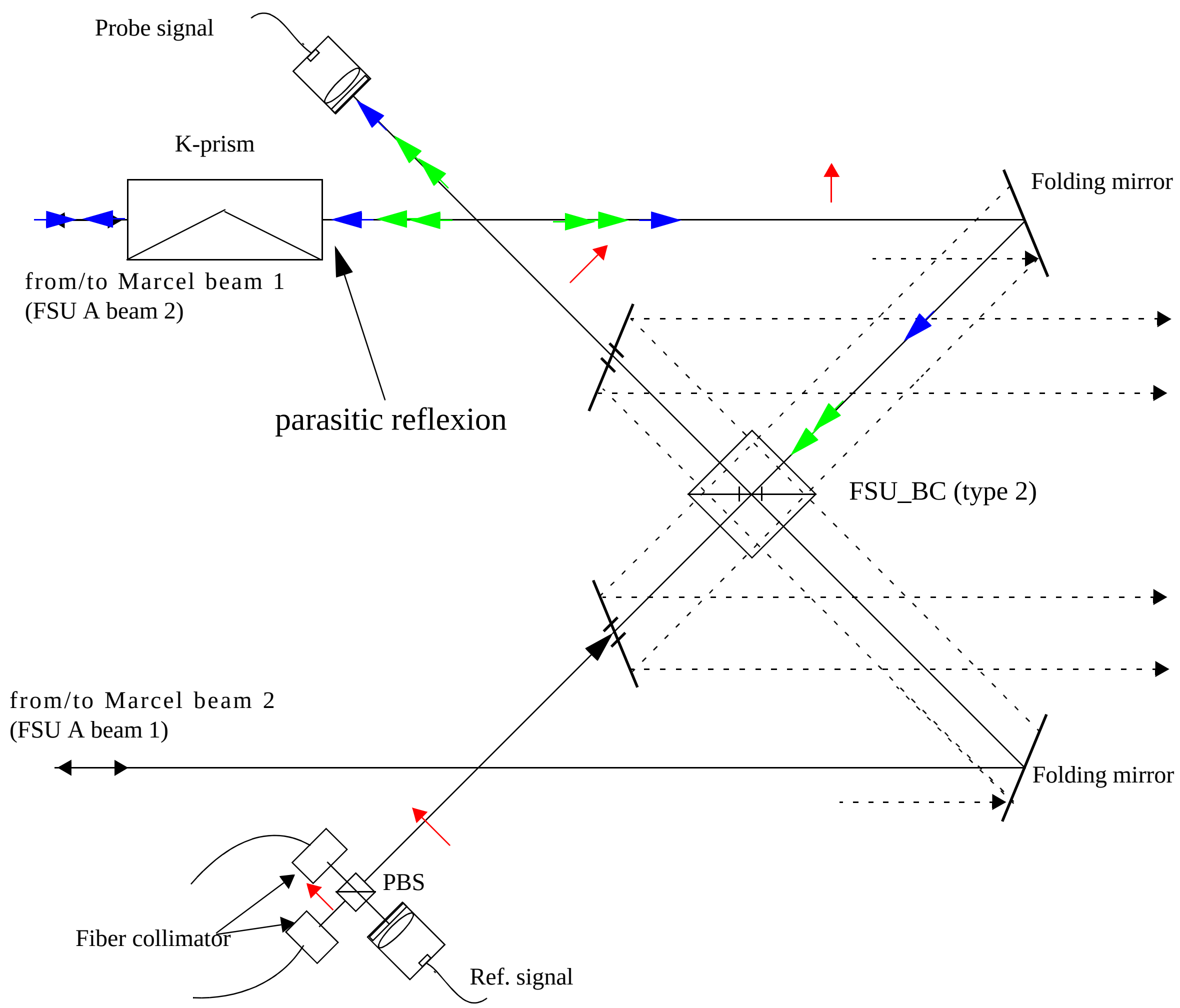

Figure 20 Schematics representing the origin of the DC variations seen on the FSU probe signal.

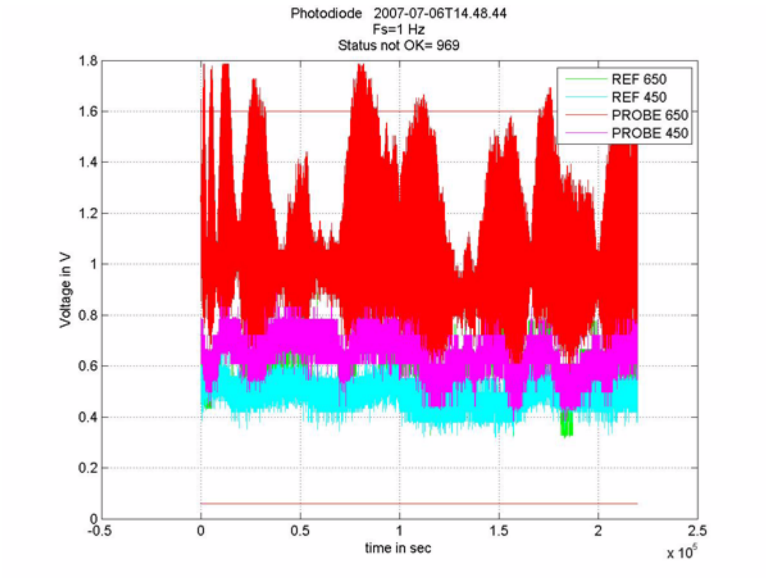

Figure 21 *DC level of the phasemeter photodiodes outputs measured over a week-end. The photodiode corresponding to the probe signal of FSU A, in red, presents large variations. These variations are caused by interferences between the nominal beam retroreflected by Marcel and the ghost created by the face of the K-prism.*

It has been shown that these variations were mainly caused by the FSU A beam 2 (polarization p, i.e transmitted through the beam combiner). Initially, it was assumed that these intensity fluctuations were caused by a misalignment between the FSU beam 1 and beam 2. However it was discovered that these variations were in fact due to interference between the nominal beam retroreflected by Marcel and a ghost created by refection on the face of the K-prism, see Figure 20.

This parasitic reflection has two consequences. First, it creates this large intensity fluctuations and add an offset to the probe signal detected by the phasemeter. This increases the chance of having not enough flux or of reaching saturation thus decreasing the robustness of the system. Secondly, it can be shown that the light reflected on the K-prism interferes with the beam coming from the other arm of the interferometer and creates a parasitic beat signal. This beat signal is responsible for an error in the phase measurement. This error is cyclic with the OPD between the K-prism face and the retro-reflector and its amplitude is proportional to the relative intensity of the parasitic beam and nominal beam.

The lens used to couple the returning beam into the multimode fiber was translated laterally w.r.t the fiber core, in order to shift the image of the ghost out of the fiber core. Unfortunately the two spots are superimposed and it was impossible to get rid of the parasitic light without decreasing significantly the power of the probe signal.

The fiber coupler uses a 5 mm focal length lens to inject the light into a multimode fiber with core diameter 65 μm. Therefore, in order to avoid coupling the light from the reflected beam, the tilt between the nominal and the ghost beam must be larger than 32.5 mm / 5 mm, i.e 6.5 mrad = 22.3 arcmin. This requires to tilt the K-prism by 11 arcmin.

The K-prism of FSU A has been tilted by inserting 0.4mm of shim between the K-prism and the alignment pin (close to the BC). This removed completely the back reflection of the k-prism into the multimode fibre but also the light coming back from MARCEL. The folding mirror of ACU and the last mirror of the testbed (before MARCEL) were tuned to recover both beam tilt and beam lateral position.

6.2.6 Reflectivity of the K-prism front surface on FSUA at 1319 nm

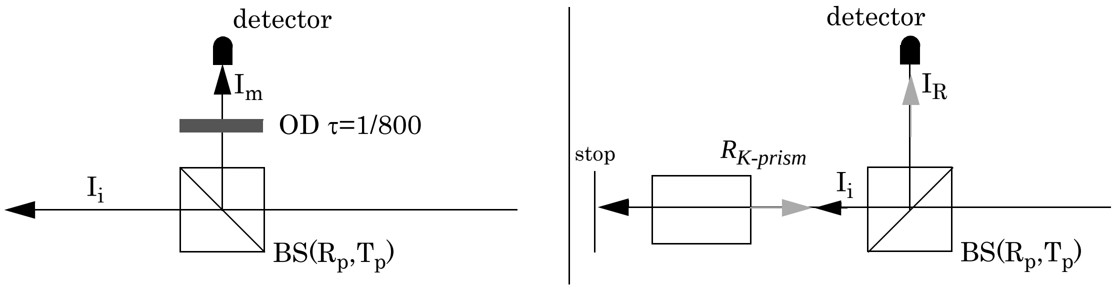

Figure 22 Two steps measurement of the K-prism antireflective coating reflectivity. The antireflective coating reflectivity is 0.23 % (specifications 0.2%).

The reflectivity of the K-prism coating has been measured. The set-up is depicted in Figure 22. The first step is to measure the power reflected by the calibrated BS in front of the K-prism. It allows to estimate the power incident on the K-prism. If one denotes:

- I_i the power incident on the K-prism;
- I_m the power measured with the an optical density of transmission τ=1/800;
- R_p=44.6%, T_p=55.4% the coefficient of reflection and transmission of the BS for the polarization p;

on has:

$$I_i = I_m \times \frac{1}{\tau} \times \frac{T_p}{R_p}. \quad (6.2\text{-}1)$$

I_m is measured to be 5.2 μw, which corresponds to incident power on the K-prism of 5.2 mW.

For the second step the BS is rotated by π/2 and the intensity of the light coming back from Marcel and reflected by the K-prism face is measured with the powermeter. The intensity measured with powermeter is fluctuating between 61 μW and 111 μW because of the interference between the two beams. If the beam is blocked after the K-prism and only the intensity reflected by the K-prism is measured, the powermeter indicates I_R = 27 μW.

I_R is equal to:

$$I_R = \frac{100}{R_p} I_i R_{K-prism} \quad (6.2\text{-}2)$$

which leads to:

$$R_{K-prism} = \frac{I_R}{I_i} \times \frac{R_p}{100} . \qquad (6.2\text{-}3)$$

$R_{K\text{-}prism}$ is measured to be 0.23% which corresponds to specifications of 0.2%.

6.3 Opto mechanical tests on FSU B

These tests provided results comparable to those presented for FSU#A

6.4 Tip/tilt stability of injection optics

The tip-tilt introduced on the metrology laser beam by the 5 axis beam launcher stage has been measured with an auto collimator. A mirror was glued on one dummy OFR fiber port. The set-up is displayed in Figure 23. The tip-tilt has been measured over 24 hour with a resolution of 0.1 arc-second and a sampling frequency of 2.85 Hz. The temperature is monitored during the whole measurement.

Figure 23 Set-up for the measurement of the tip-tilt created by the 5 axis stage.

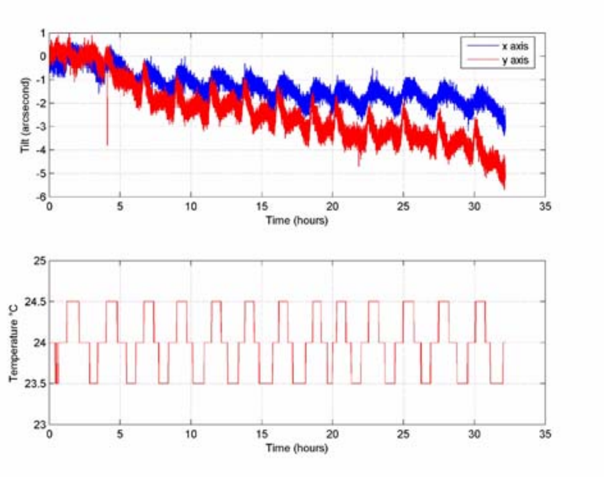

Figure 24 *Tip-tilt introduced by the 5 axis stage on the laser metrology beam. The measurements are done with an autocollimator on a mirror glued on a dummy fiber port (similar to the one used for the injection optics). The resolution of the autocollimator is 0.1 arcsecond and the sampling frequency about 2.85 Hz.*

The tip-tilt measured is the sum of the tip-tilt caused by the 5-axes stage, the autocollimator mount and the breadboard deformation. The tip-tilt reaches a peak-to-peak value of 6 arcsecond. The loss of fringe contrast due to such a tip-tilt can be neglected.

7 Phase Meter

The phase meter as been tested as reported in RD 8. The performance summary are indicated in the following figure. The accuracy value includes the contribution of the overall metrology electronic chain, i.e including the AOM, detectors...etc.

During the test period in Garching, the firmware of the phase meter has been updated as reported in RD 11. A new backplane has been integrated in the phase meter as described in RD 9.

Phase resolution / Range	
Differential phase	Resolution: $2\pi/1024$ or 0.6 nm
	Range: $2^{29} \cdot 659.5\,\mathrm{nm}/1024 = 346\,\mathrm{mm}$
Phase compensation	2π or 659.5 nm
	Range: $2^{24} \cdot 659.5\,\mathrm{nm} = 11\,\mathrm{m}$
Sampling frequency	
Internal (instantaneous phase)	200 kHz
External (accumulated phase)	0.36 Hz–15 kHz
Maximum OPL speed of DL and DDL ($v_{OPLmax} = \lambda\, \Delta\nu/2$)	
DL	
Specs: $450, 650\,\mathrm{kHz} \pm 55\,\mathrm{kHz}$	$\pm 36\,\mathrm{mm/s}$
As built: $450, 650\,\mathrm{kHz} \pm 75\,\mathrm{kHz}$	$\pm 49\,\mathrm{mm/s}$
DDL	
Specs: $200\,\mathrm{kHz} \pm 27.5\,\mathrm{kHz}$	$\pm 18\,\mathrm{mm/s}$
As built: $200\,\mathrm{kHz} \pm 34.5\,\mathrm{kHz}$	$\pm 23\,\mathrm{mm/s}$
Noise of the photodetectors	
$-128\,\mathrm{dBm/Hz}$ or NEP $= 0.14\,\mathrm{pW}/\sqrt{\mathrm{Hz}}$	
Phase difference introduced by the bandpass filters (p. 23)	
< 0.42 deg or $2\pi/857$ or 0.8 nm (peak).	
Noise level of the digital phasemeter (p. 29)	
(for 7 nW equivalent optical power, rms over 50 Hz–50 kHz.)	
0.8 dig or $2\pi/1280$ or 0.5 nm.	
Phase difference introduced by the movement of the DL	
(including the phase difference introduced by the bandpass filters, see above)	
Phasemeter "Spare 1"	$2\pi/256$ or 2.6 nm (limited by the set-up)
Phasemeter "Spare 2" σ_1=	$2\pi/426$ or 1.5 nm ←
Accuracy	
σ_2= $2\pi/800$ or 0.8 nm (rms) over OPL = 180 mm. ←	

Figure 25 *Phase meter performance summary*
The total error is sqrt($\sigma_1^2+\sigma_2^2$)=1.7nm rms

8 Pupil tracker.

The test of the pupil tracker is reported in RD 6.

Additional tests were conducted in May 2008 at Paranal on STS-AT#4. Preliminary results indicates that the specification are met while operating on a short light duct. Measurements were performed on the G2 maintenance station, with DL#2 at OPL=14 m. In addition the enclosure of AT#1 and AT#2 were opened to increase air circulation inside VLTI (external wind speed ~ 8 m/s).

The residuals were dominated by a 46 Hz eigen frequency whose origin has not been yet determined. The pure delay of the system was 20msec compared to 15 msec measured in Garching. The difference may come from the fact that the vcm was connected to its pressure chamber at Paranal using a rigid "tube", thus changing the dynamic response of the VCM. Investigations are in progress.

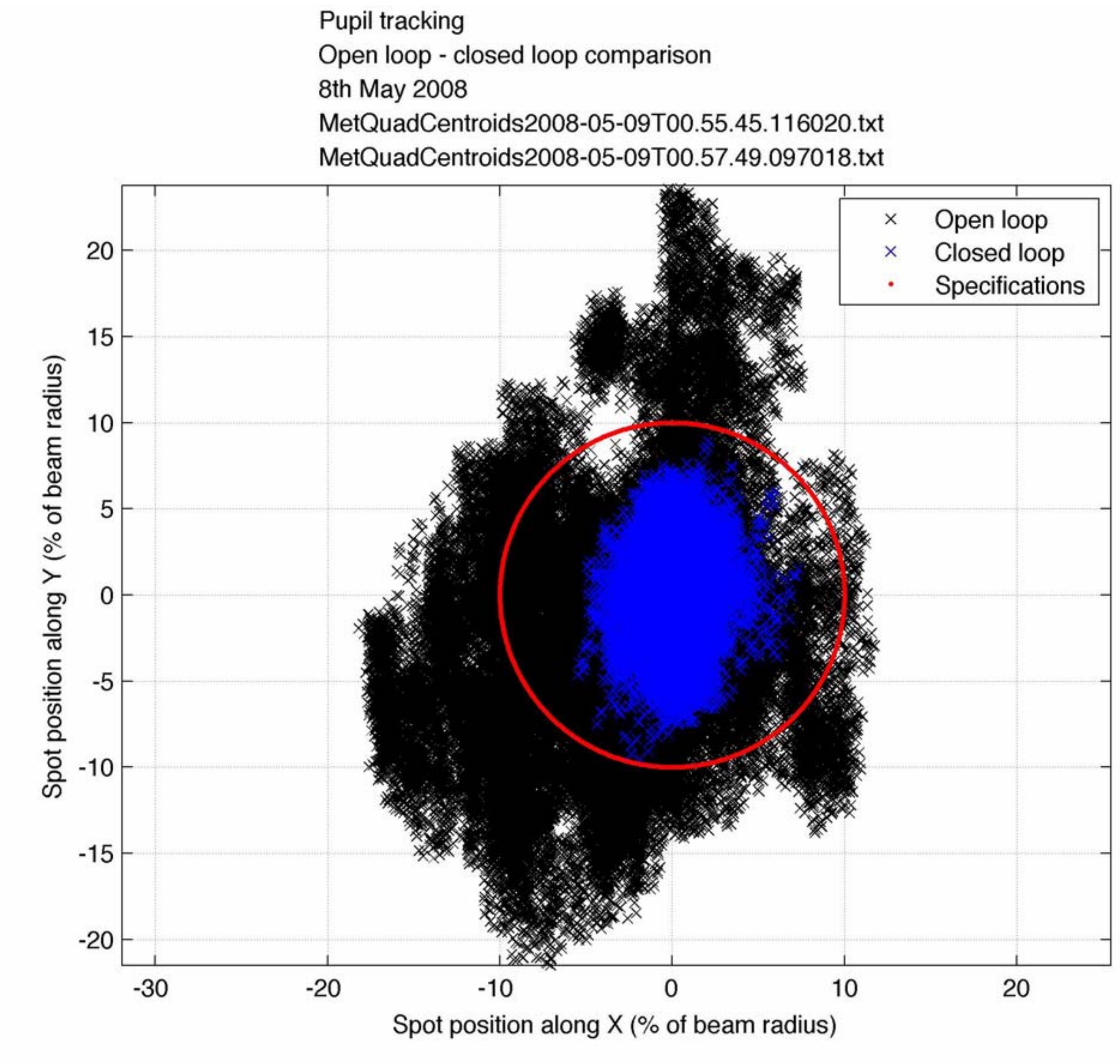

Figure 26 Laser Beam centroid position measured by a 4 quadrant detector located on the PRIMA 2 table. Open-loop and closed-loop positions are recorded during 1min in each case with a sampling frequency of 1 kHz and a correction frequency of 100 Hz. The closed loop bandwidth of the system is 2.5 Hz.

9 Control Hardware

The PRIMET control hardware consists in 4 LCU's and several drivers ad controllers as described in RD 9. This hardware is located in three electronics cabinets.

The control hardware has been tested in the PRIMA Fringe Tracking Testbed.

A list of problems that were encountered and their associated remedies are given in appendix.

10 Control Software

10.1 Verification of the specified software features

All the features described in RD 10 and RD 4 have been implemented and tested on the testbed. Problems were reported in the form of VLT SPR's.

10.2 Automatic data logging

The automatic data logging as defined in RD 10 has been implemented and tested. The logfile generated by wprima can be quickly analysed using the script PRIMETLOG located in the directory /data/PRIMETDATA/ on WPRIMA. The file produced by wprima (name format "wprima.YYYY-MM-DD.log") must be copied first into the directory /data/PRIMETDATA/. Then the script can be executed with the command:

sh PRIMETLOG wprima.YYYY-MM-DD.log PRIMETLOG.YYYY-MM-DD.log

It generates a file "PRIMETLOG.YYYY-MM-DD.log“ summarizing the logging on commands and special events generated by lprmac, lprma2 and lprmls.

A copy of the script is given in the appendix of this document.

11 Impact of the phase screens

A set of phase screens (glass disk engraved with a phase map coded on 32 bits, 100 microns pixels) had been manufactured to simulate the residual wave front errors of the UT MACAO system. They can be introduced in one arm of the interferometer of the testbed. A motor is used to rotate the disk and model time dependent aberrations. The effect of these aberrations on the metrology have been tested. However, it should be noted that these phase screens are not representative of the reality for the metrology beam. Indeed, the metrology beam is not affected by the MACAO system. Moreover the phase screens have been designed to work for 18 mm diameter beams in K band in single pass configuration whereas, on the testbed, the metrology beam diameter is at most a few millimeters and propagates twice through the phase screen.

One phase screens is mounted in FSU B (beam 1, polarization s) as close as possible to Marcel. It is put close to Marcel to be as close as possible to the pupil plane of the system defined by the

MARCEL metrology retroreflectors. The phase screen is rotated. Only light polarized along s is launched in the interferometer. The DC signal on the reference and probe photodiodes of the phasemeter are recorded. An example is shown in Fig. 27. One can clearly see that the metrology signal extracted from the FSU presents fast variations in time and sometimes reaches 0. When the p polarization is used simultaneously with the s polarization, the resulting beat signal is unstable and the contrast can drop to 0 which causes a glitch.

Unfortunately this could not be avoided on the testbed. Matlab simulations have confirmed the experimental results. The poor quality of the metrology beam when used with the phase screen is due to:

- the reduced beam diameter compared to the one used for the design of the PS;
- the double pass configuration.
- there is no pupil plane defined in the testbed

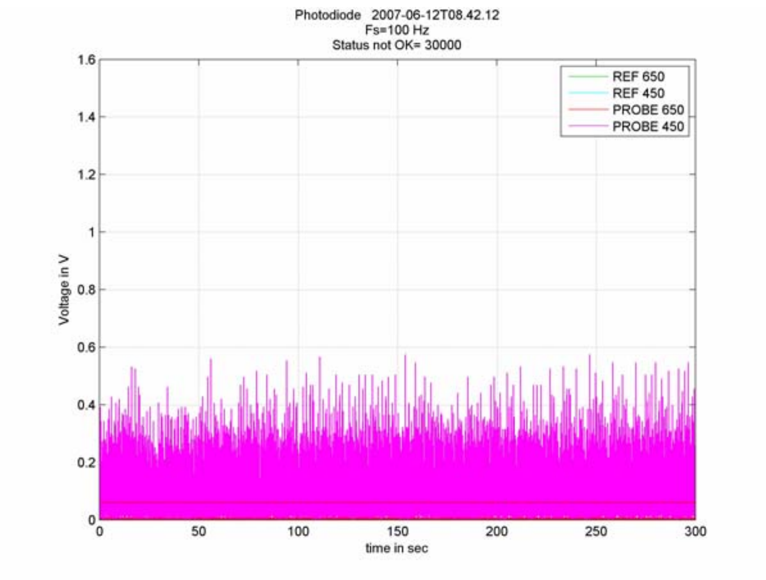

Figure 27 *Voltages of the photodiodes of the phasemeter when light is propagated on the FSU B beam 1 in which is introduced a rotating phase screens (Top: full sequence; Bottom: zoom).One can see that the probe signal is extremely noisy and drops sometimes to 0 which in the presence of the other signals would create a glitch.*

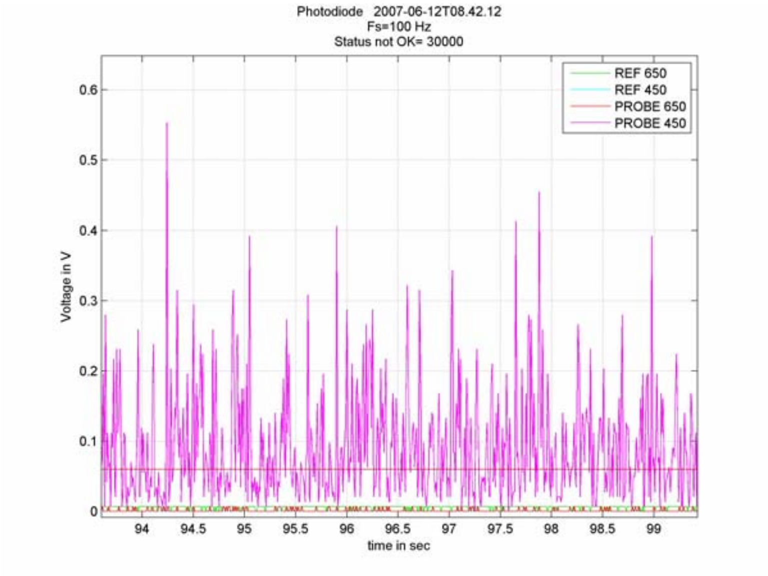

Figure 27 *Voltages of the photodiodes of the phasemeter when light is propagated on the FSU B beam 1 in which is introduced a rotating phase screens (Top: full sequence; Bottom: zoom).One can see that the probe signal is extremely noisy and drops sometimes to 0 which in the presence of the other signals would create a glitch.*

12 Laser Straylight on the FSU detectors

The straylight measurements carried out on FSU B have been done in a worst case configuration for which the laser light is propagated towards the FSU using MARCEL. The laser light incident on the FSU occupies the full 18mm pupil instead of the central 2mm patch. The set-up used is presented in Figure 28. During the measurements the FSU detector integration time is 2 s. The pump diode current in the Nd:YAG laser is 1.307 A. The intensity is measured in beam 1 and 2 of MARCEL before the FSU ACU by focusing the laser beam on the Newport powermeter detector. The intensity is 0.67 mW in beam 1 and 0.6 mW in beam 2. Before the measurement the injection in the FSU is optimized using the beam tracking procedure with MARCEL fed by the halogen lamp.

4 full frames of the detector have been saved:

- background (no laser light);
- beam 1 and beam 2 simultaneously;
- beam 1 only;
- beam 2 only.

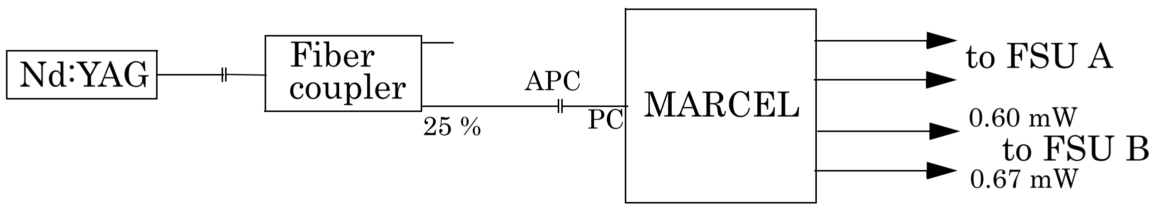

Figure 28 Set-up for the measurement of the laser metrology straylight on the FSU.

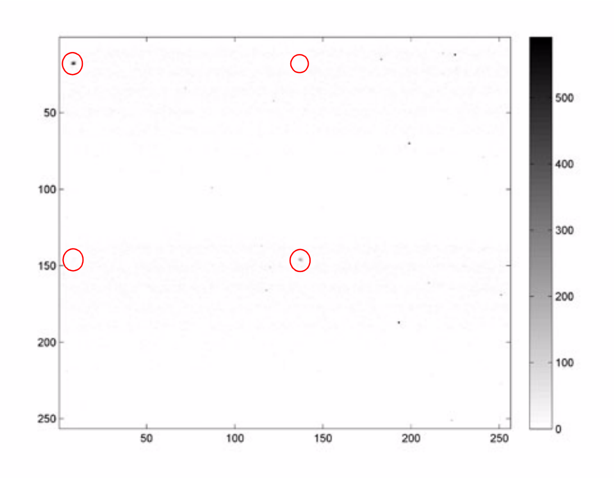

Figure 29 *Straylight measured on the FSU B. The laser light, injected with MARCEL, covers the full pupil. The power in both incoming beams is around 0.630 mW which is about 1000 times the power expected to come back from the telescope. The straylight is mostly visible on two channels out of four.This may be explained by the polarization of the laser light and or by the interference.*

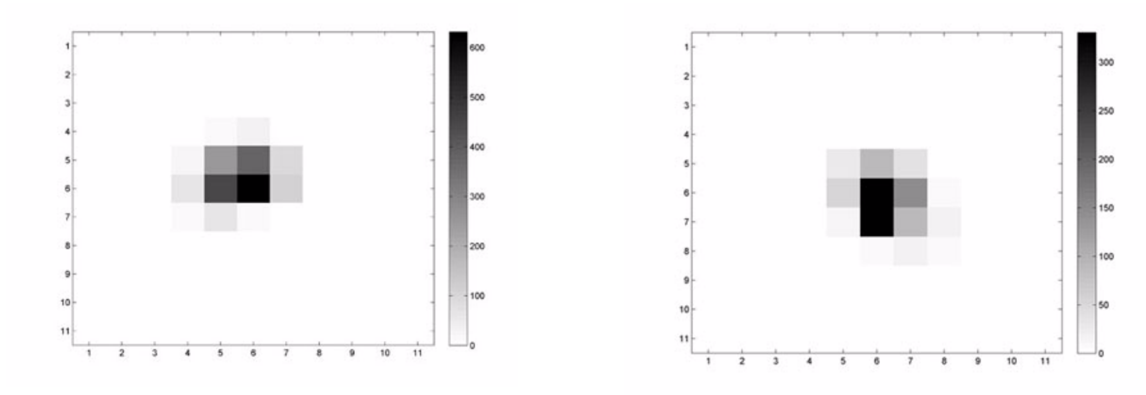

Figure 30 *Close-up of the two spots created by the laser straylight. The peak intensity corresponds to 600 ADU for an integration time of 2 s.*

The straylight of the metrology laser is mostly on two channels out of the four. This is due to the presence of interference and/or to the polarization of the laser light. Due to the wavelength mis-matched between the stellar light and the laser light, the image of the straylight is out of focus and covers several pixels instead of one. The maximum straylight on one pixel corresponds to 600 ADU for a two second exposure for an incident power of 0.6 mW per beam. For a 1 s exposure and for an incident flux of 0.5 μW per beam, as expected during operation, the straylight amounts to 0.3 ADU, i.e 2.7 electrons. This is to be compared to 2700 electrons of thermal background.

One can also estimate the transmission of the FSU at 1319 nm. The total incident power on the FSU during the measurement is 1.27 mW. The sum of the straylight in the four channels is about

3400 ADU, corresponding to 6.24 fW. Therefore the transmission of the FSU can be estimated to be 5×10^{-12}.

13 OPD recorded on the testbed

The PRIMA metrology has been extensively used to characterize the FSU as reported in RD 12 Some example of OPD recorded by the metrology are given below

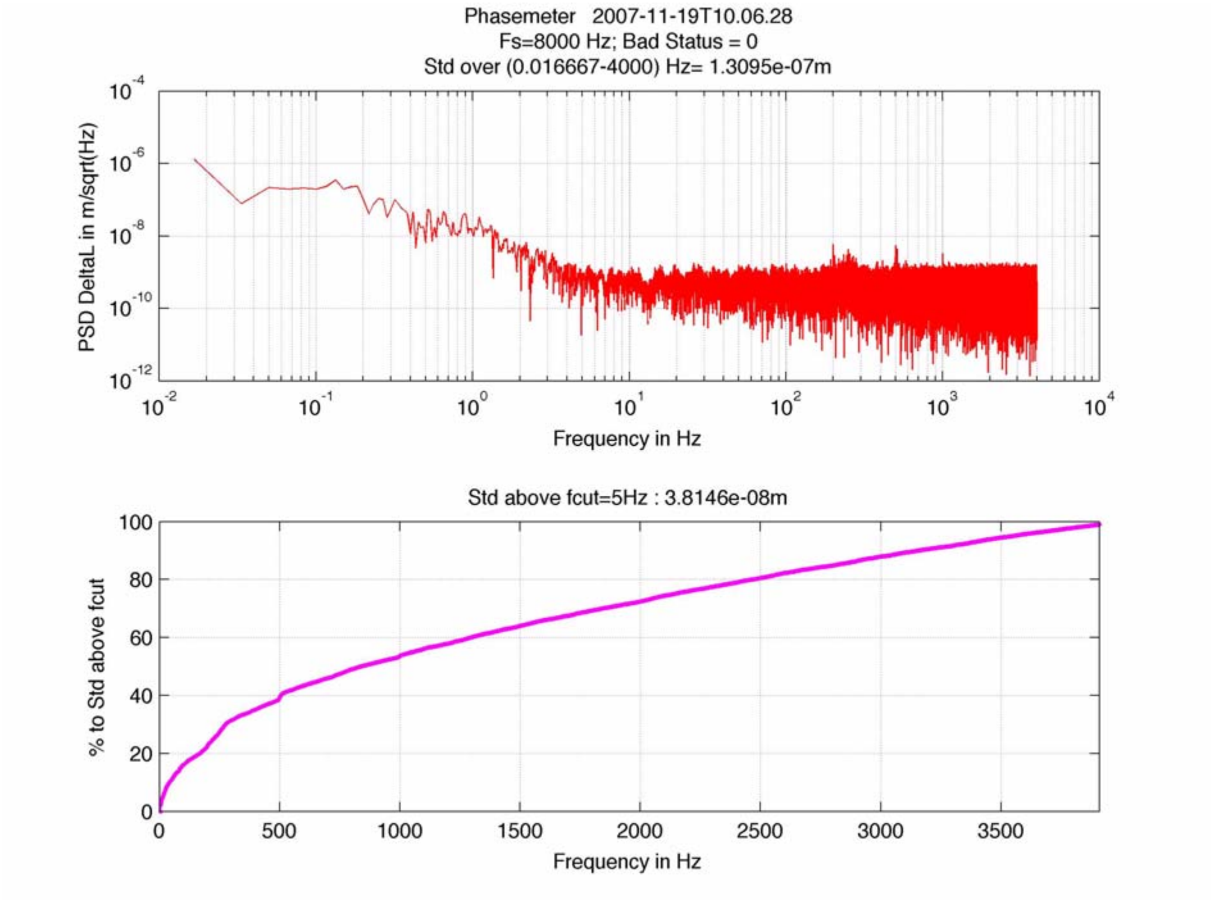

Figure 31 OPD measured by the metrology on the testbed. All loops are open. The OPD reflects the stability of the testbed.

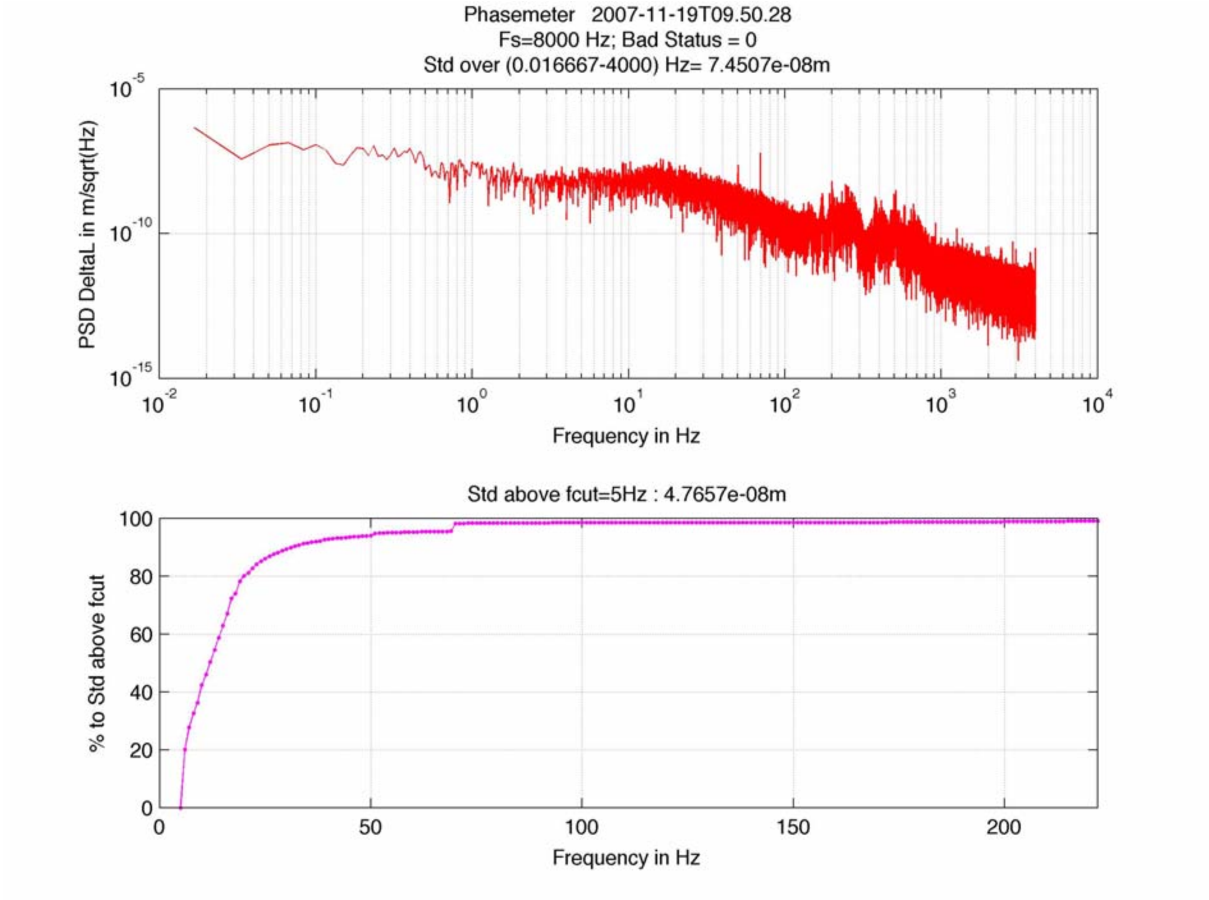

Figure 32 Residuals measured by the metrology with IFG ON (i.e. atmospheric tip tilt corrections), and FSU NOT tracking. The “standard” atmospheric tip/tilt is injected by a tilt mirror and corrected by the FSU ACU (IFG)

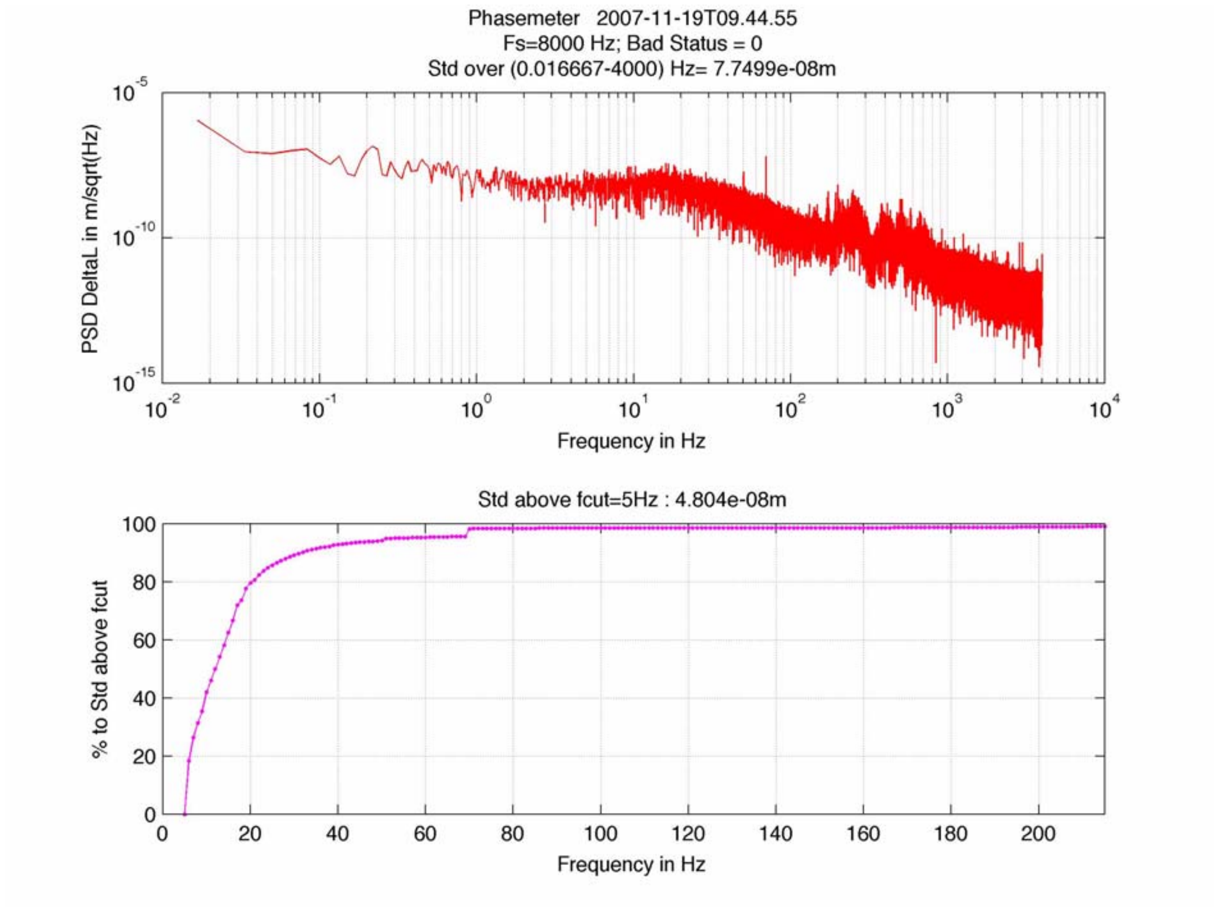

Figure 33 Residuals measured by the metrology with IFG ON (i.e. atmospheric tip tilt corrections), and FSU tracking. The "standard" atmospheric tip/tilt is injected by a tilt mirror and corrected by the FSU ACU (IFG)

14 PRIMET BENCH MARK: Performance summary

The measured performance of the PRIMA metrology are highlighted herebelow.

Table 9 shows that the error on ΔL is limited to 5.35 nm rms but excluding the contribution of the non-common optical path. At this stage it is not possible to give a quantitative estimate of this contribution.

Table 10 summarizes the measured system performance.

Table 9 Error budget for ΔL

Source of error	Value	Reference
Laser Head		
Frequency stability 10^{-8} (for 0.6 nm rms ΔL= 60 mm) and Absolute accuracy of the Laser wavelength: 10^{-8} (0.6 nm rms for ΔL= 60 mm)	sqrt(2).0.6= 0.85 nm rms	RD 7
Electronics		
Heterodyne assembly, Fiber relay, Phase meter	1.7 nm rms	RD 8, section 7
Optical Configuration		
Polarization Cross-talks	5 nm rms	section 6.2.4
TOTAL (uncorrelated, without non common path contribution)	**5.35 nm rms**	

Table 10   PRIMA Metrology measured System performance

Parameters	**Value**
ΔL Noise	0.5 nm
ΔL Resolution	0.6 nm
ΔL Accuracy	5.35 nm ([1])
Maximum ΔL speed	dΔL/dt <+/- 27 mm.s^{-1}
Sampling frequency	8kHz ([2])
ΔL Range (before wrapping)	346 mm
Operating Wavelength	λ=1319nm
Laser Frequency Stabilization	dν/ν<10^{-8}
Straylight on the FSU detector	2.7 e^{-} ([3])
Pupil Tracking residuals	10% of the beam radius ([4])

1. excluding non-common path errors
2. The maximum sampling frequency of ΔL provided by the phase meter is 15kHz. However, the metrology control software uses a maximum value of 8kHz.
3. this value is 1000 less than the thermal background
4. this corresponds to 100 µm for a 1mm beam radius

15 Appendix

15.1 Script for the analysis of PRIMET automatic logging

name of the file: PRIMETLogAnalyser
Syntax: PRIMETLogAnalyser InputLogFilename.log OutputResultsFilename

```
cat >$2 << EOF
/*****************/
/PRIMETLOG SUMMARY/
/*****************/
EOF

cat >>$2 << EOF

/***********************/
/Phasemeter A-B (lprmac)/
/***********************/

REFMET
EOF
grep lprmac $1 | grep 'REFMET1' | wc -l >> cat >>$2
grep lprmac $1 | grep 'REFMET1' >> cat >>$2

cat >>$2 << EOF

RESET
EOF
grep lprmac $1 | grep 'RESET1' | wc -l >> cat >>$2
grep lprmac $1 | grep 'RESET1' >> cat >>$2

cat >>$2 << EOF

DATANOTVALID
EOF
grep lprmac $1 | grep 'DATANOTVALID1' | wc -l >> cat >>$2
grep lprmac $1 | grep 'DATANOTVALID1' >> cat >>$2
```

```
cat >>$2 << EOF

PMOVFL
EOF
grep lprmac $1 | grep 'PMOVFL1' | wc -l >> cat >>$2
grep lprmac $1 | grep 'PMOVFL1' >> cat >>$2

cat >>$2 << EOF

FCOVFL
EOF
grep lprmac $1 | grep 'FCOVFL1' | wc -l >> cat >>$2
grep lprmac $1 | grep 'FCOVFL1' >> cat >>$2

cat >>$2 << EOF

WRNGLOWFLUX
EOF
grep lprmac $1 | grep 'WRNGLOWFLUX' | wc -l >> cat >>$2
grep lprmac $1 | grep 'WRNGLOWFLUX' >> cat >>$2

cat >>$2 << EOF

WRNGSAT
EOF
grep lprmac $1 | grep 'WRNGFSAT' | wc -l >> cat >>$2
grep lprmac $1 | grep 'WRNGFSAT' >> cat >>$2

cat >>$2 << EOF

/*********************/
/Phasemeter B (lprma2)/
/*********************/

REFMET
EOF
grep lprma2 $1 | grep 'REFMET2' | wc -l >> cat >>$2
grep lprma2 $1 | grep 'REFMET2' >> cat >>$2

cat >>$2 << EOF

RESET
```

```
EOF
grep lprma2 $1 | grep 'RESET2' | wc -l >> cat >>$2
grep lprma2 $1 | grep 'RESET2' >> cat >>$2

cat >>$2 << EOF

DATANOTVALID
EOF
grep lprma2 $1 | grep 'DATANOTVALID2' | wc -l >> cat >>$2
grep lprma2 $1 | grep 'DATANOTVALID2' >> cat >>$2

cat >>$2 << EOF

PMOVFL
EOF
grep lprma2 $1 | grep 'PMOVFL2' | wc -l >> cat >>$2
grep lprma2 $1 | grep 'PMOVFL2' >> cat >>$2

cat >>$2 << EOF

FCOVFL
EOF
grep lprma2 $1 | grep 'FCOVFL2' | wc -l >> cat >>$2
grep lprma2 $1 | grep 'FCOVFL2' >> cat >>$2

cat >>$2 << EOF

/**********************/
/Frequency Stabilization/
/**********************/

LASERPOWER
EOF

grep lprmls $1 | grep 'LASERPOWER' | wc -l >> cat >>$2
grep lprmls $1 | grep 'LASERPOWER' >> cat >>$2

cat >>$2 << EOF

DATANOTVALID
EOF
grep lprmls $1 | grep 'LOOPPARAM' | wc -l >> cat >>$2
```

```
grep lprmls $1 | grep 'LOOPPARAM' >> cat >>$2

cat >>$2 << EOF

PMOVFL
EOF
grep lprmls $1 | grep 'AUTOPHASE' | wc -l >> cat >>$2
grep lprmls $1 | grep 'AUTOPHASE' >> cat >>$2

cat >>$2 << EOF

INNOLIGHTNOTOK
EOF
grep lprmls $1 | grep 'INNOLIGHTNOTOK' | wc -l >> cat >>$2
grep lprmls $1 | grep 'INNOLIGHTNOTOK' >> cat >>$2

cat >>$2 << EOF

FREQLOOPUNSTABLE
EOF
grep lprmls $1 | grep 'FREQLOOPUNSTABLE' | wc -l >> cat >>$2
grep lprmls $1 | grep 'FREQLOOPUNSTABLE' >> cat >>$2

cat >>$2 << EOF

INNOLIGHTTECERROR
EOF
grep lprmls $1 | grep 'INNOLIGHTTECERROR' | wc -l >> cat >>$2
grep lprmls $1 | grep 'INNOLIGHTTECERROR' >> cat >>$2
```

```
more $2
```

15.2 Problem reporting and tracking during the testing period

Table 11

Problem Reporting and tracking

Description	Status	Owner	Comments
Control HW/SW			
ISER12 board cannot read device	closed	RFR	conflict with new version of driver
Stabilization and phase meter cannot operate in parallel Measurement LCU needs “frequent” reboot	closed	RFR/SLE	Measurement and stabilization plit in 2 LCU
Metrology data on RMN are corrupted	Closed	RFR	Conflict of address of the boards of the metrology LCU
RESET PM generates different status depending on sampling frequency	Closed	NSC	Solved by implementing new Firmware
Status Phase meter toggle red after STOPMET/STARTMET			
time of Eng file wrapps after given time	Closed	RFR	increase nb of bits for the time
Robustness of Innolight switch ON/OFF using DO	Closed	SLE/RFR	correct software implementation done
1/3/07 Number of samples in 14 whatever the sampling frequency Jump in the number of samples (similar to connection problem of DIO conector)			
Phase Meter			
Backplane of digital Phase Meter loose connection (1 bit of 6x 32 bit word corrupted after thermal cycle) Photodiode DC signal noisy	Closed	SLE/AJO	Backplane Redesigned
1024 digits phase jumps	Closed	SLE/YSA	New firmware version of the Phase meter (see RD 11)

Table 11

Problem Reporting and tracking

Description	Status	Owner	Comments
spare3 phase meter : status dead	Closed	SLE	Spare 2 sent by YSL as replacement Spare1: used in lprmac Spare2: used in lpma2
phase meter always delivers data (although no clear signal at 5 V)	Closed	SLE	OR Gate NC7S32 after Clear input was dead. New gate purchased and replaced.
Clear signal not always detected in Status delivered by Phase meter	Closed	SLE	Bug in Phase meter Firmware (10/06) (see RD 11)
Large amplitude modulation on the photodetectors signal	Closed	SLE	1/ cross-talk FSUA/FSUB. Signals are mixed on the fiber of Marcel 2/ noise eater of innolight only works with specific input current. At lower power, amplitude modulation actually amplified by AOM (see below)
Laser Frequency Stabilization			
Error signal <<100mV	Closed	NSC	new alignment of frequency stabilization optics
Interlock triggered by noise on interlock cable	Closed	SLE	Capacitance inserted on interlock input of the driver to filter the noise
Overload on the lock-in	Closed	SLE	The noise eater of the innolight laser works only for a given current level. At lower power, some intensity noise (actually amplified by AOM) is generated. The laser head should always be operated at its nominla power. Tuning of the power shall be done using the AOM driver